Self-Assembled Monolayers Protecting Metal Nanoparticles

3-D SAMs

Outline

- **Introduction to nanoparticles**
- **Monolayer-Protectected Metal nanoparticles**
  synthesis, characterizations
  properties and packing of the monolayer
- **Functional Nanoparticles**
  Methods of synthesis. Mixed-monolayers
  Monovalent- and divalent metal nanoparicles
- **Nanoparticles of different size and shape**
- **Applications of nanoparticles in different fields**

NANOPARTICLES

books

Colloidal Gold. Principles. Methods, and Applications
M. A. Hayat, 3 volumi, Academic Press, 1989

Nanoparticles. From Theory to Application Edited by Günter Schmid
Wiley-VCH, 2004

Metal Nanoparticles: Synthesis, Characterization, and Applications.
Edited by D. L. Feldheim and C. A. Foss; M. Dekker, Inc., 2002.

reviews

Self-Assembled Monolayers of Thiolates on Metals as a Form of Nanotechnology
J. C. Love, L. A. Estroff, J. K. Kriebel, R. G. Nuzzo, G. M. Whitesides, *Chem. Rev.* **2005**, *105*, 1103.

Large Clusters and Colloids. Metals in the Embryonic State
G. Schmid, *Chem. Rev.* **1992**, *92*, 1709.

Chemistry Change with Size
C. N. R. Rao, G. U. Kulkarni, P. J. Thomas, P. P. Edwards, *Chem. Eur. J.* **2002**, *8*, 29.

On the development of colloidal nanoparticles towards multifunctional structures and their possible use for biological applications
T. Pellegrino, S. Kudera, T. Liedl, A. Muñoz Javier, L. Manna, W. J. Parak, *Small*, **2005**, *1*, 48.

…….and thousands of papers

A brief historical background

- gold nanoparticles are known since ancient time, 5º - 4º millenium B.C. (China, Egypt). We believe that ancient Egyptian known how to prepare "soluble" gold and they were used these solutions as "elisir".

- colloidal gold sols are used to obtain red glass

- around 1600 Paracelso (1493-1541) described the preparation of "aurum potable, oleum auri: quinta essentia auri" by reduction of acid tetrachloroauric using an alcoholic extract of plants.

  At that time medical doctors believed that "drinkable gold" exert curative properties for several diseases.

A brief historical background

The roman industry of IV century A.D., developed a sophisticated use of metal NPs, they were able to produce colored glass with particular optical properties.
For example the addition of Ag and Au compounds, enable to produce glass which appear to be green under reflected light and red under trasmitted light.
The famous "Licurgus cup" has been realized with this technique.

day light (reflected light) trasmitted light

40 ppm of Au and 300 ppm of Ag

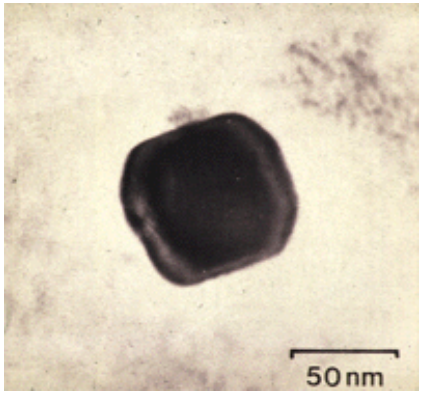

TEM image

Nanoparticles - hystorical background

- in 1857 Michael Faraday reported the first scientific studies on preparations of colloidal gold solutions, M. Faraday, *Phil.Trans.Roy. Soc.* **1857**, *147*, 145.
- around the half of 19th century the italian physician Enrico Selmi write a description of "colloids", not very different from the actual definition.
- in 1861 the term "**colloid**" (from the greek *kolla)* was conied by the Scottish chemist Thomas Graham

$(AuCl_4)^-$ —white phosphorous, reduction on CS_2→ solution of colloids

diameter of 3 ÷ 30 nm

two phase system

Nanoscale Materials

Florence - Santa Croce

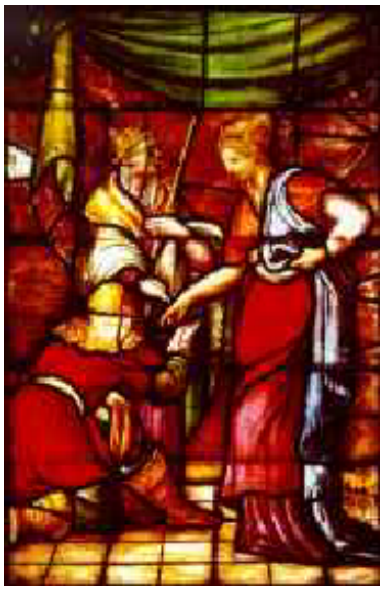

Milan - Duomo

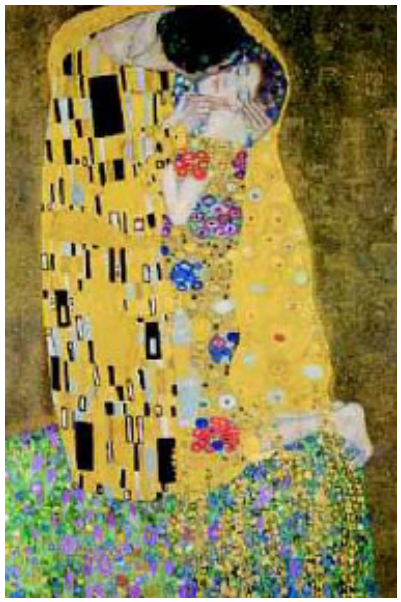

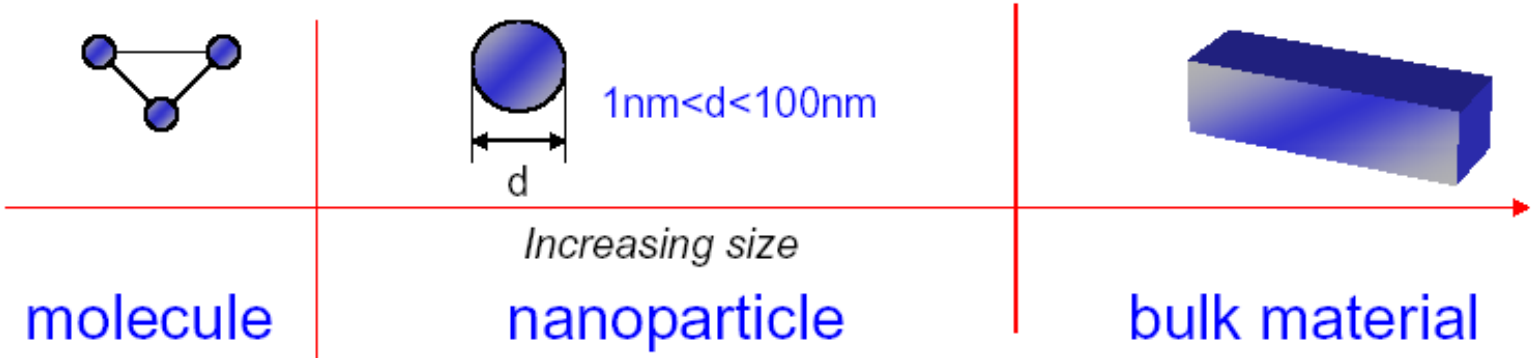

Nanoscale materials have different properties when compared to their bulk counterparts!

Nanoscale Materials

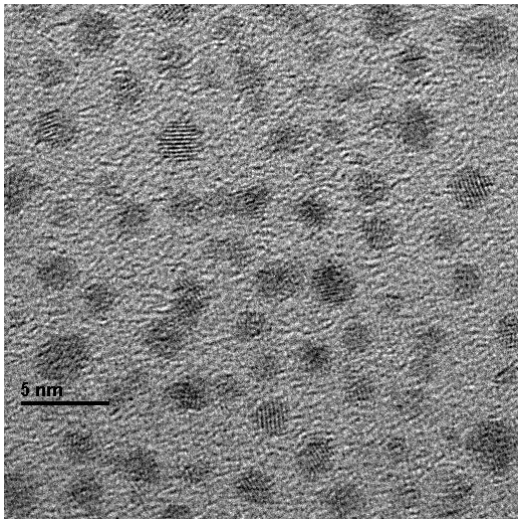

Nanoparticles - quantum dots

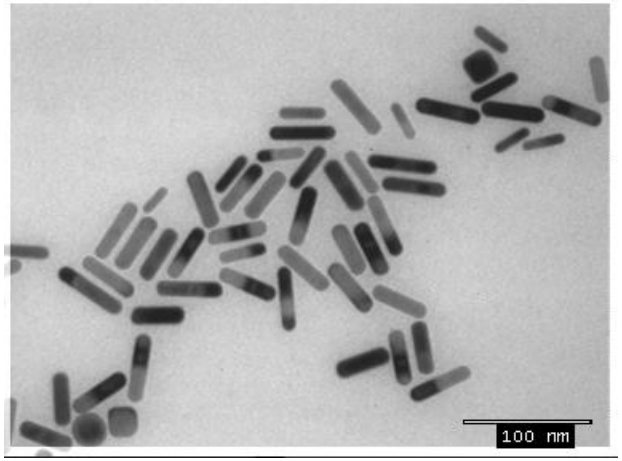

nanorods

0 dimensional nanomaterials:
unique properties due to
quantum confinement
and very high surface/volume ratio

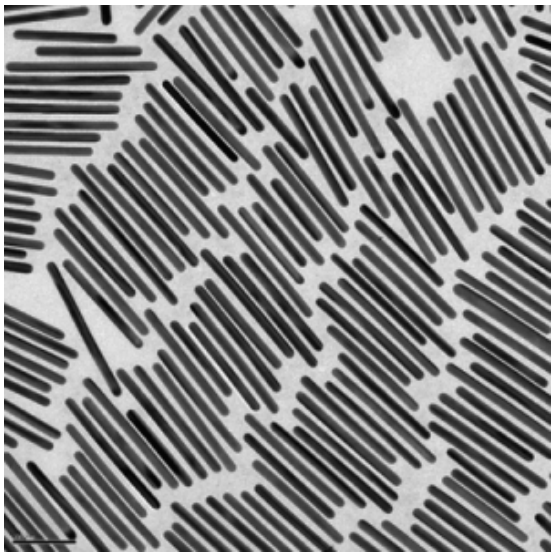

nanowires

1 dimensional nanomaterials:
extremely efficient
classical properties

These ultra-long devices exhibit tremendous photothermal properties, converting up to 90% of incident light energy to heat.

Properties of Metal Nanoparticles

Optical Properties

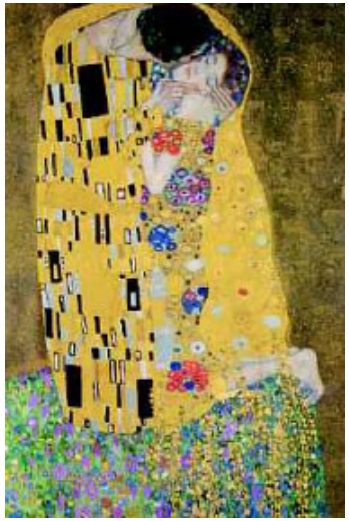

Electronic Properties

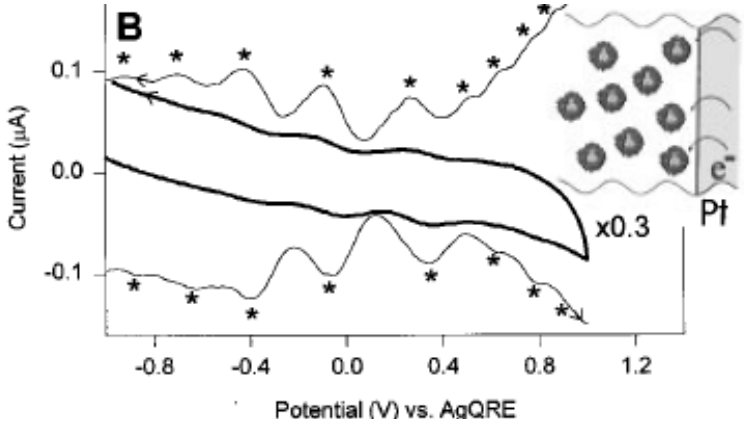

Nanoscale Materials Have Different Properties when compared to their bulk counterparts!

Nanoscale Materials

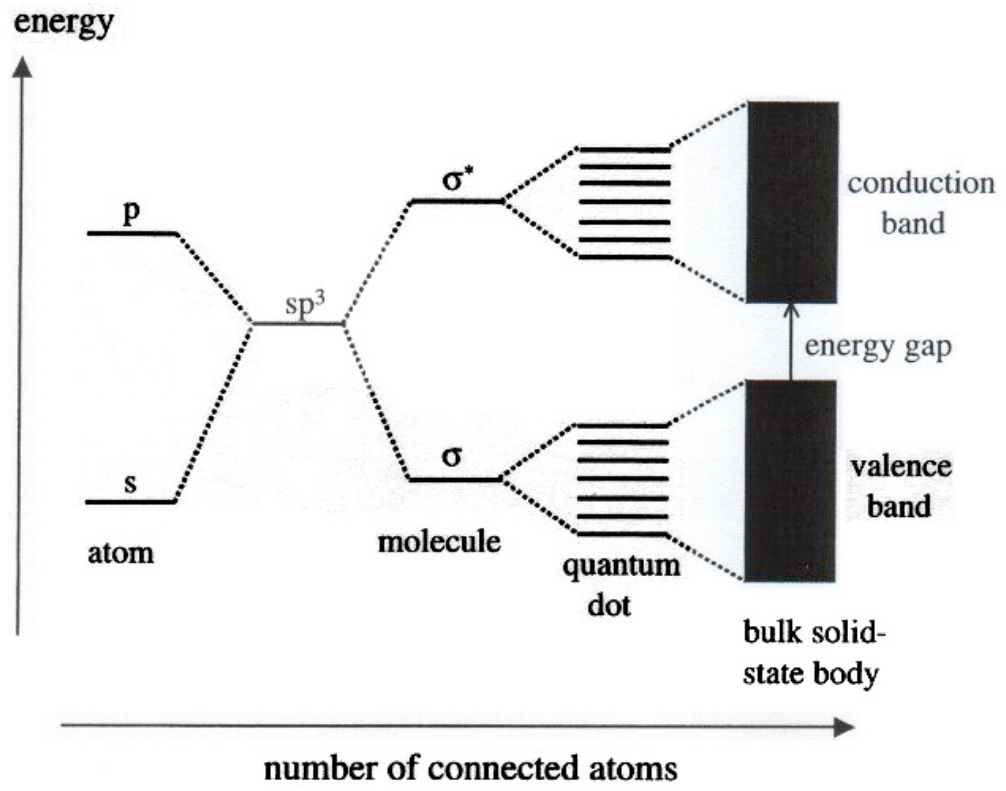

Fig. 2-1 Electronic energy levels depending on the number of bound atoms. By binding more and more atoms together, the discrete energy levels of the atomic orbitals merge into energy bands (here shown for a semiconducting material) [16]. Therefore semiconducting nanocrystals (quantum dots) can be regarded as a hybrid between small molecules and bulk material.

Synthesis of metal nanoparticles

PVD *(physical vapor deposition)*

formation of clusters in the gas phase - Au metal as strating material

for example, the nanoparticles are formed from bulk metal by irradiating it with a laser beam.
At low laser flux, the material is heated by the absorbed laser energy and evaporates
or sublimates and deposited over a solid support, under UHV condition.

es. cathodic arc deposition, sputter deposition, electron beam physical vapor deposition, laser ablation

CVD *(chemical vapor deposition)*

organometallic compounds as starting material

In a typical CVD process, the wafer (substrate) is exposed to one or more volatile precursors,
which react and/or decompose on the substrate surface to produce the desired deposit.
Frequently, volatile by-products are also produced, which are removed by gas flow through
the reaction chamber.

problem: control of the NP size

Synthesis of metal nanoparticles

- control of size, shape and composition with synthetic methodologies that allows to produce significative quantities of NPs.

- **molecular approach to colloidal metals**: use of molecular precursors

- many of the known methods are applicabile to different metallic elements of the periodic table, for exemple the reduction with hydrides.

- colloidal NPs are unstable and aggragate if not stibilized

Synthesis of metal nanoparticles

Two methods against aggregation:

- **electrostatic stabilization**
- **steric stabilization**

- 12-64 nm J. Turkevitch, P. C. Stevenson, J. Hillier, *Disc. Farady Soc.* **1951**, *11*, 55.

Reduction with **sodium citrate** developped by Frens in 1973:
this is the most used method for the preparation of gold colloids.

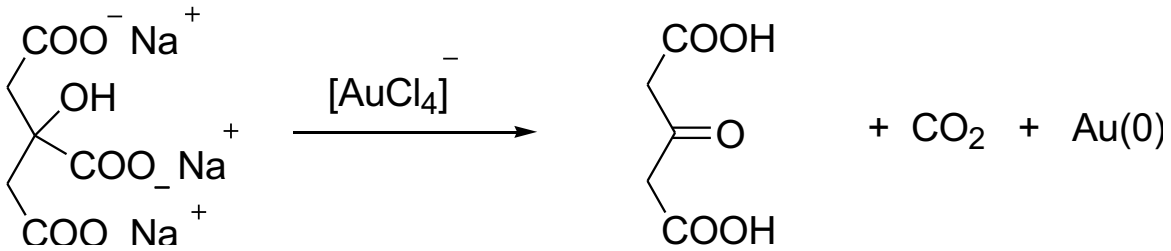

it is easy
•it requires only water
•it requires skills
•has reproducibility issues

NPs size may increases using more diluted solutions.

Synthesis of metal nanoparticles

Electrostatic stabilization: the electrical double layer

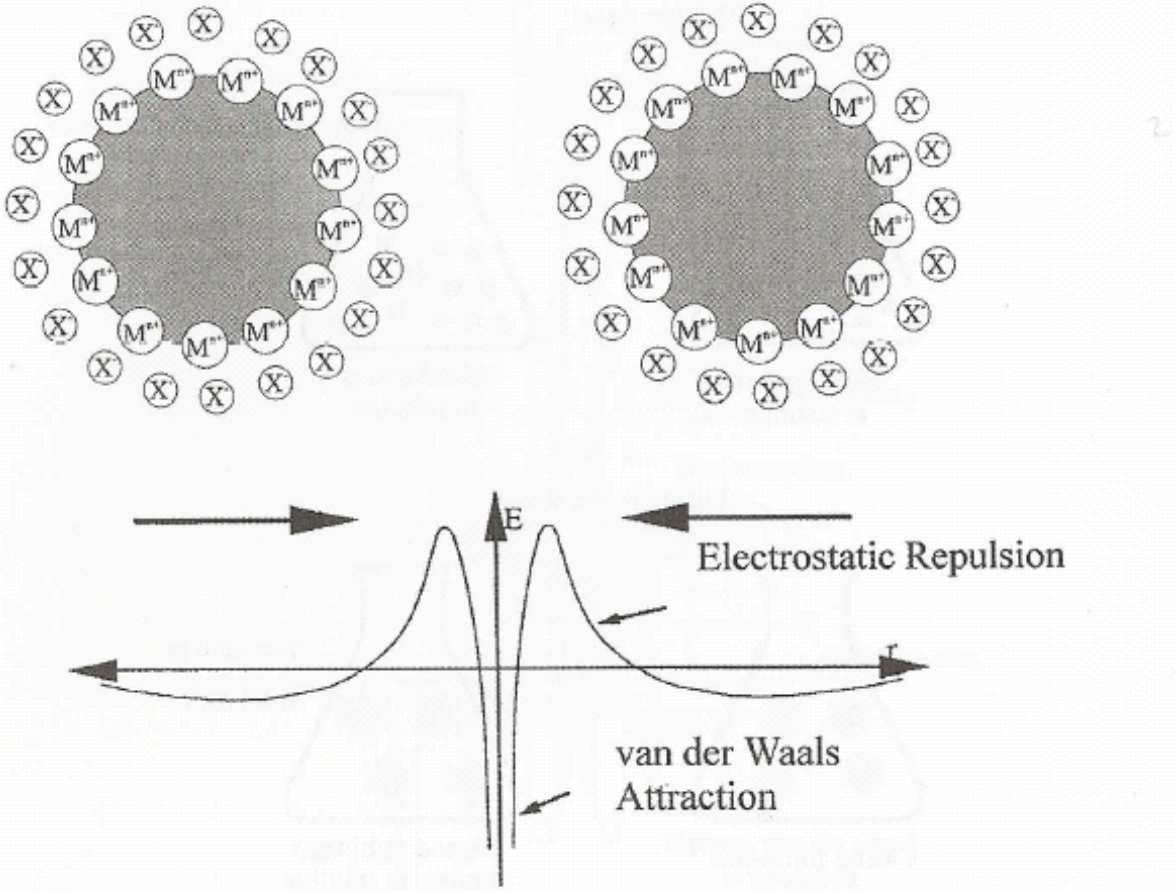

FIGURE 2.24 Electrostatic stabilization of metal colloids. Van der Waals attraction and electrostatic repulsion compete with each other.[27]

the energetic maximum can be easily overtake increasing for example the ionic strength or by increasing the thermal movement of the NPs.

Synthesis of metal nanoparticles

reduction of $HAuCl_4$ with different reducing agents

- 3-4 nm sodium borohydride ($NaBH_4$)
- 12 nm

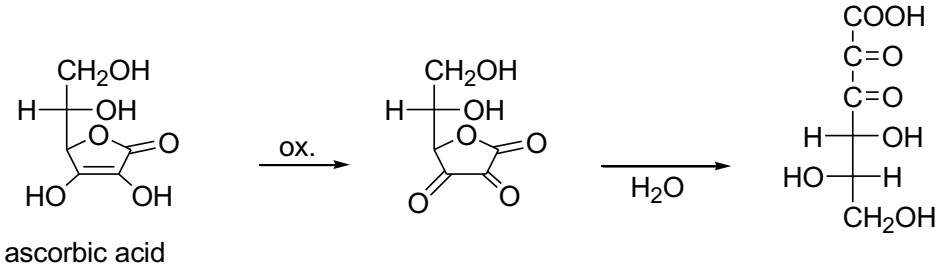

ascorbic acid

- 12-64 nm

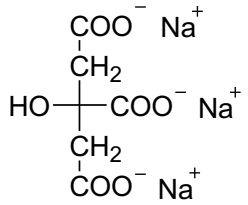

sodium citrate

Synthesis of metal nanoparticles

- the strength of the reducing agent determine the NP size
- the reaction conditions are also very important in determining the average diameter
  - the size may be reduced by: increasing reductant
    decreasing volume
    increasing stirring
    increasing temperature

Synthesis of metal nanoparticles

Steric stabilization

polymers, surfactants, and legands may be used to form a protective monolayer

polymers: they should present specific groups that bound to the NPs surface

Gold Number: quntity of polymer that stabilize 1 g of a solution of
50 mg/L of colloidal gold against aggregation in the presence of NaCl 1%

PVP [poly(vinylpyrrolidone)] and **PVA**, poly(vinyl alcohol) o
CTAB (cetyltrimethilammonium bromide)

These polymers have been used also to stabilize Pt and Ag NPs

Synthesis of metal nanoparticles

reduction of transition metals salts

- by using solvents that may easily be oxidized as alcohols that are oxidized to aldehydes or ketones

- Hirai and Toshima, "alcohol reduction process" and polymers for the stabilization

$$RhCl_3 + 3/2\ R_1R_2CHOH \longrightarrow Rh(0) + 3/2\ R_1R_2C{=}O + 3\ HCl$$

Other reducing agents:

Ascorbic acid, hydrogen, formaldehyde, hydrazine

Characterization of NPs

TEM *(transmission electron microscopy): give information about structure Dimension, dispersion, shape, and composition of the metal core*

HRTEM si ottengono informazioni sulle distanzi interplanari, TEM in alta risoluzione.

HAADF-STEM high-angle annular dark-field imaging in the scanning electron microscope
è una tomografia elettronica adatta ad analizzare nanomateriali cristallini

X-ray diffraction

XRD

SAXS small-angle X-ray scattering (down to 1 nm)
anomalous SAXS (synchrotron radiatio)

WAXS wide-angle X-ray scattering

EXAFS extended X-ray absorption fine structure

XPS X-ray photoelectron spectroscopy

Mössbauer spectroscopy

XANES X-ray absorption near-edge structure

STS *scanning-tunneling spectroscopy*

Transmission Electron Microscope (TEM)

TEM
Copenhagen - 200 kV

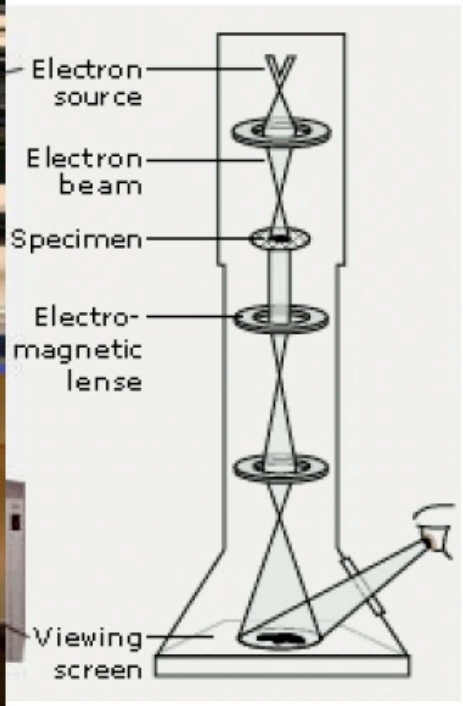

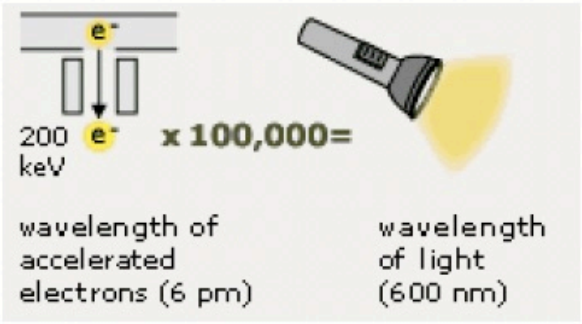

	Optical	TEM
Radiation	*Light*	*Electrons*
Lenses	*Glas*	*Magnetic fields*
Wavelength	*ca. 0,5 µm*	*ca. 2 picometer*
Resolution	*ca. 0,5 µm*	*0,1 - 0,2 nm*
Sample thickness	*ca. 25 - 50 µm*	*ca. 10 - 200 nm*

- Å resolution
- *Transmission*,
  ie only thin slices

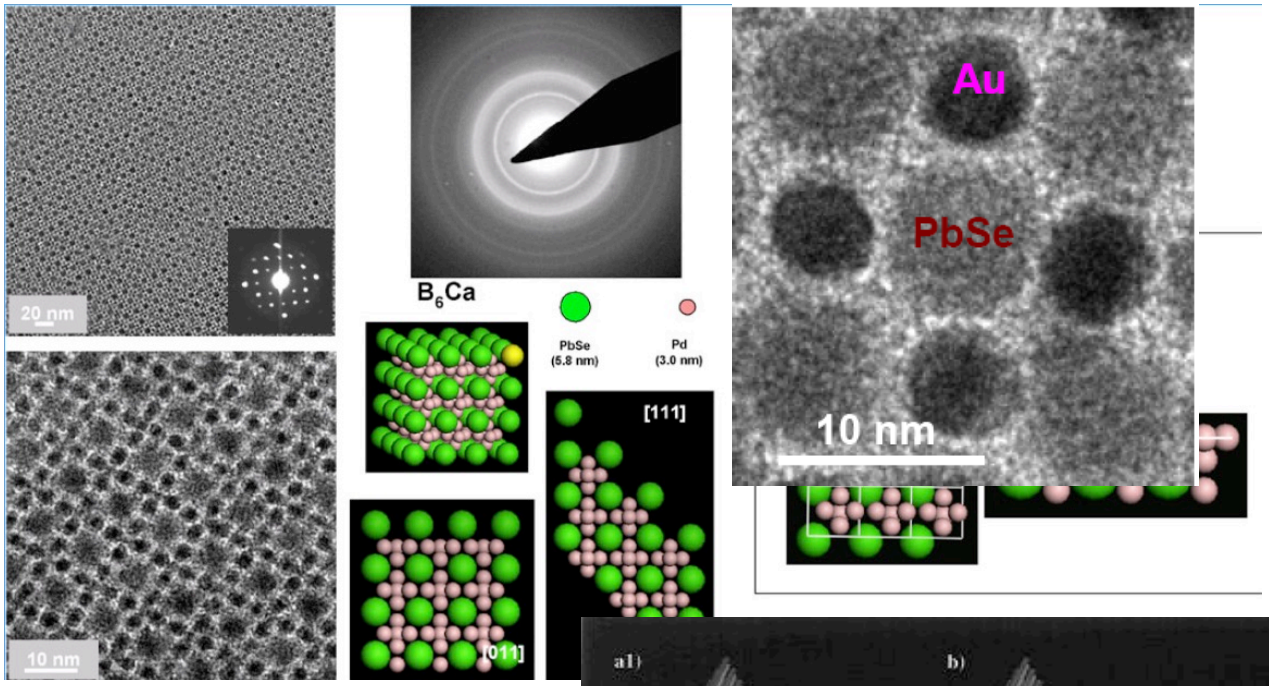
20 nm
10 nm
B6Ca
PbSe
(5.8 nm)
Pd
(3.0 nm)
[111]
[011]
Au
PbSe
10 nm

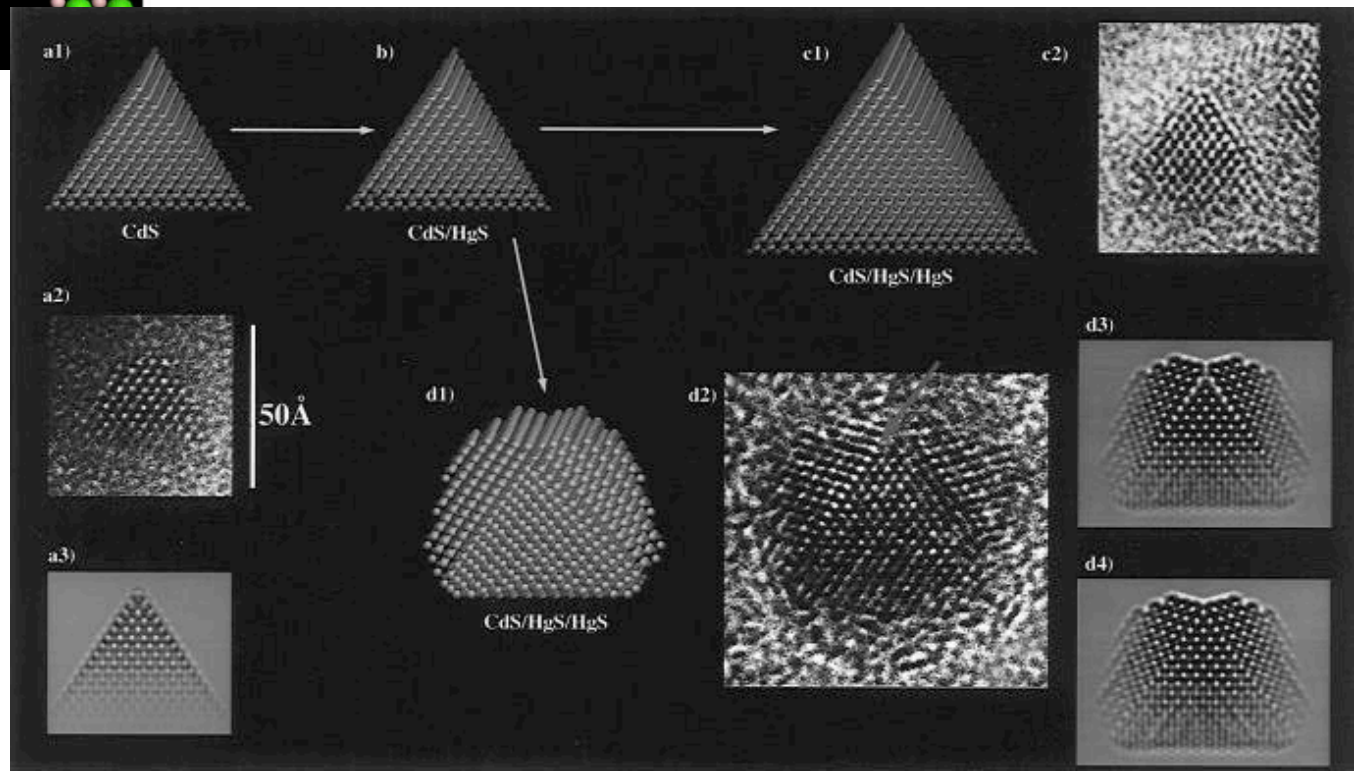
a1)
b)
c1)
c2)
CdS
CdS/HgS
CdS/HgS/HgS
a2)
50Å
d1)
d2)
d3)
a3)
CdS/HgS/HgS
d4)

NANOPARTICELLE - SINTESI

Au, Pd, Pt,

full-shell clusters: clusters are like onions, each atom like to complete his coordination

for metals the coordination number is 12

the first full-shell cluster is composed of 1+12 = 13 atoms

the shell *n*th includes $10n^2 + 2$ atoms

***n* shell**	1	2	3	4	5	6	7	8	9	10
n. atoms last shell	12	42	92	162	252	362	492	642	812	1002
n. total atoms	13	55	147	309	561	923	1415	2057	2869	3871
% surface atoms	92.3	76.4	62.6	52.4	44.9	39.2	34.8	31.2	28.3	25.8
average d (nm)		1.4	1.9	2.0	2.8	3.0			4.4	4.6

UNDECAGOLD

Step 1. $HAuCl_4 + 2PPh_3 + H_2O \xrightarrow[\text{or THF}]{\text{EtOH}} Ph_3PAuCl + Ph_3PO + 3HCl$

Step 2. $Ph_3PAuCl + NaBH_4 \xrightarrow[\text{or THF}]{\text{EtOH}} \boxed{Au_{11}(PPh_3)_7Cl_3}$

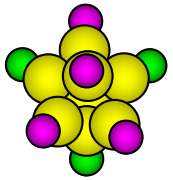

Step 3. $Au_{11}(PPh_3)_7Cl_3 + \sim 30CH_3(CH_2)_{11}SH \xrightarrow{\text{THF}} Au_{11\text{-}13}(PPh_3)_x(SC12)_yCl_z$

Step 4. Column chromatography to remove PPh_3O, Ph_3PAuCl, $[CH_3(CH_2)_{11}S]_2$

"undecagold" derivatives have been widely used as markers of biological compounds and for histochemical analysis

P. A. Bartlett, B. Bauer, S. J. Singer, *J. Am. Chem. Soc.* **1978**, *100*, 5085.
F. Cariati, L. Naldini, *Inorg. Chim. Acta*, **1971**, *5*, 172.

UNDECAGOLD

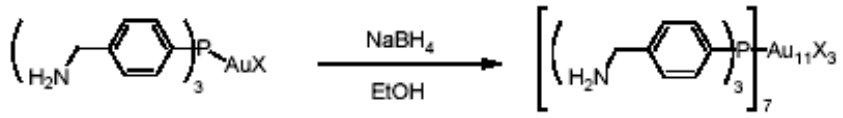

2a X = I
2b X = CN

3a X = I
3b X = CN

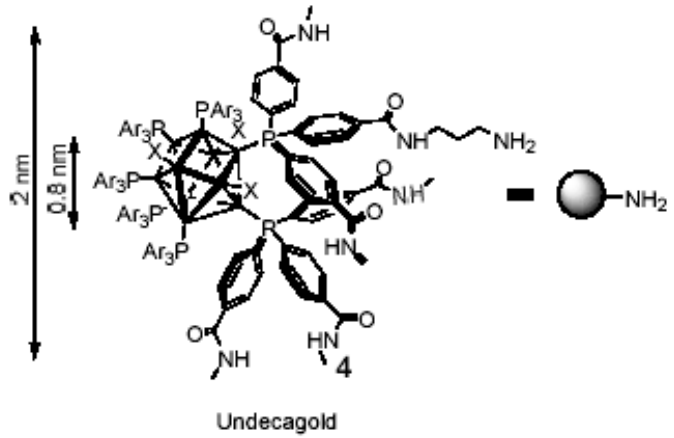

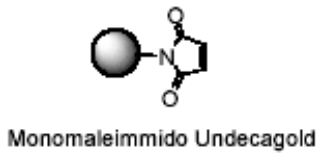

to bound thiols

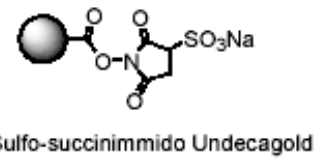

it reacts with amines

H. Yang, P. A. Frey, *Biochemistry*, **1984**, *23*, 3849, 3857, 3863.

- conjugates of peptide, ATP, nucleic acids, lipids, phospholipidis, carbohydrates, antibodies, etc. have been prepared.

Au_{55}

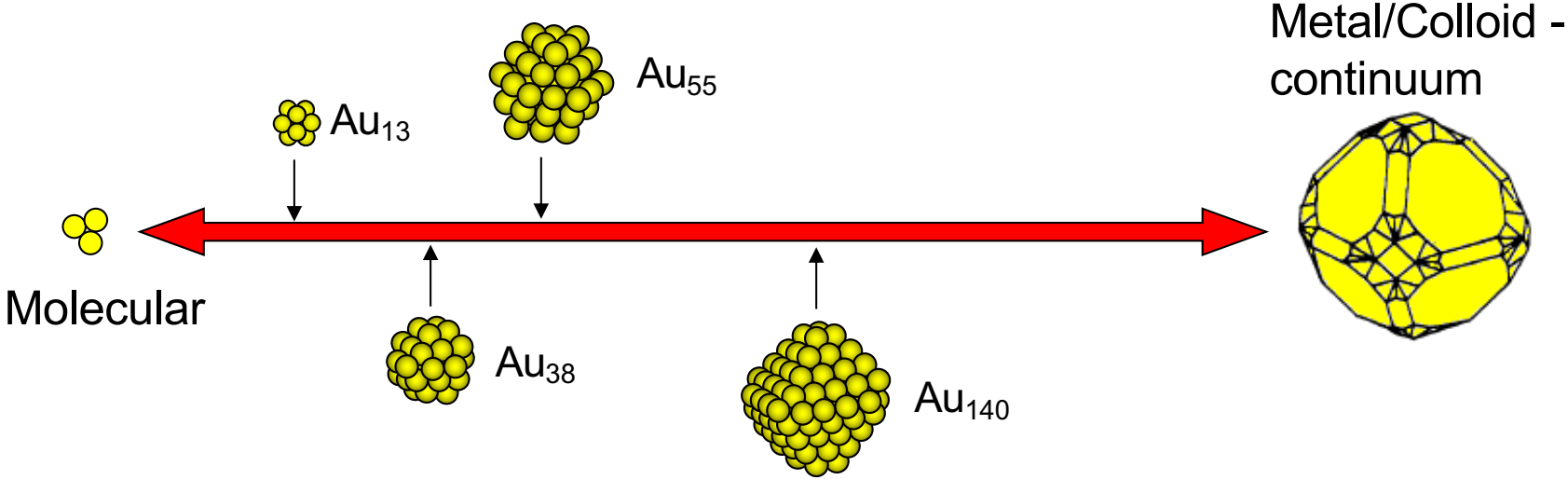

$Au_{55}(PPh_3)_{12}Cl_6$ is the most studied full-shell cluster since it represent a transition between molecular and colloidal behaviour

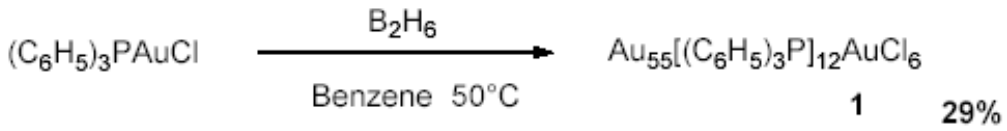

the syntheic method enable one to obtain a monodispersed cluster and because of this it could be used in the formation of fcc 3D crystals .

G. Schmid, P. Pfeil, R. Boese, F. Bandermann, S. Meyer, G. H. M. Calis, J. W. A. van der Velden, *Chem. Ber.* **1981**, *114*, 3634.

Au_{55}

Chromatographic Isolation of "Missing" Au55 Clusters Protected by Alkanethiolates

Hironori Tsunoyama,† Yuichi Negishi,† and Tatsuya Tsukuda*,†,‡

J. Am. Chem. Soc. **2006**, *128*, 6036.

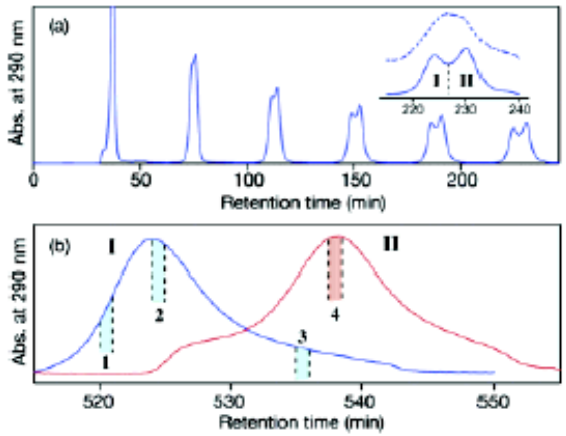

Figure 1. (a) Chromatogram of recycling GPC of the Au:SC_{18} clusters. Dotted curve in the inset is the data for the sample without etching treatment. (b) Recycling chromatograms of two fractions **I** and **II**.

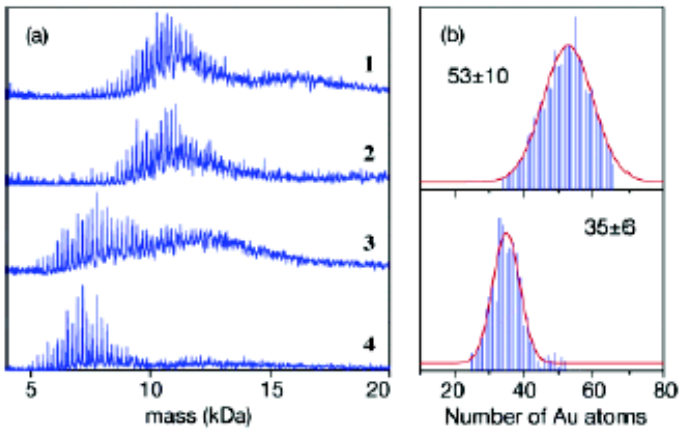

Figure 2. (a) LDI mass spectra of fractions **1**−**4** in the positive ion mode. (b) Histograms of the core numbers for fractions **2** and **4**.

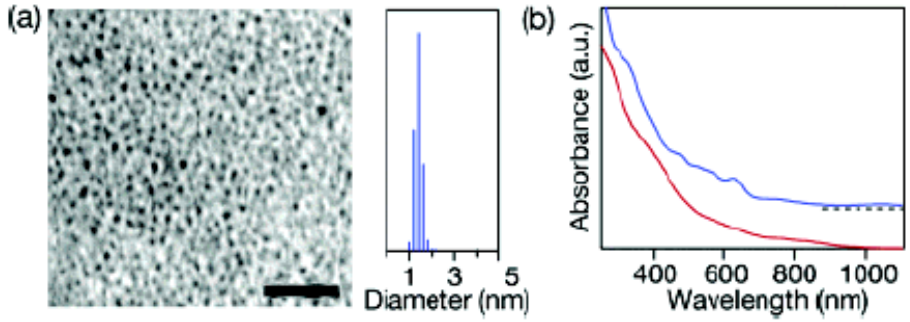

Figure 3. (a) TEM image and core-size distribution of Au_{55}:SC_{18}. The scale bar represents 20 nm. (b) Optical absorption spectra of Au_{55}:SC_{18} (red) and the 8 kDa clusters (blue).

Monolayer protected clusters MPCs

J. CHEM. SOC., CHEM. COMMUN., 1994

Synthesis of Thiol-derivatised Gold Nanoparticles in a Two-phase Liquid–Liquid System

Mathias Brust, Merryl Walker, Donald Bethell, David J. Schiffrin and Robin Whyman

Department of Chemistry, The University of Liverpool, PO Box 147, Liverpool, UK L69 3BX

Using two-phase (water–toluene) reduction of $AuCl_4^-$ by sodium borohydride in the presence of an alkanethiol, solutions of 1–3 nm gold particles bearing a surface coating of thiol have been prepared and characterised; this novel material can be handled as a simple chemical compound.

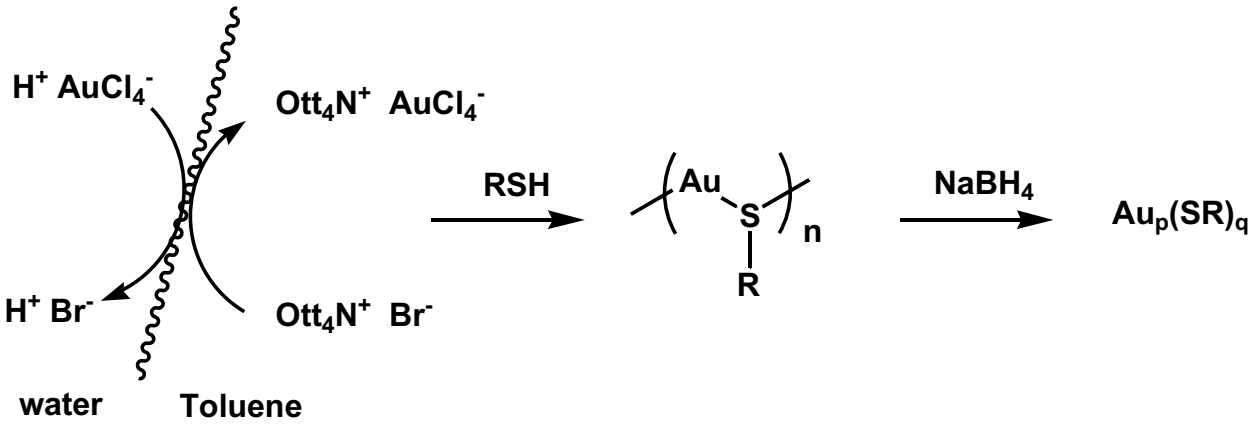

➡ MPCs OF DIFFERENT SIZE MAY BE OBTAINED USING DIFFEREN REACTION CONDITIONS:

- RATIO RSH/Au
- REDUCTION RATE
- TEMPERATURE

Nanoparticles – Au_{140}

the core

Au_{140}

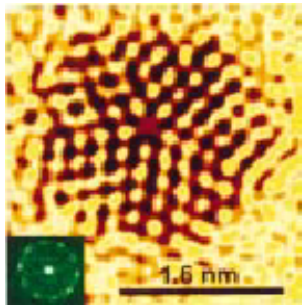

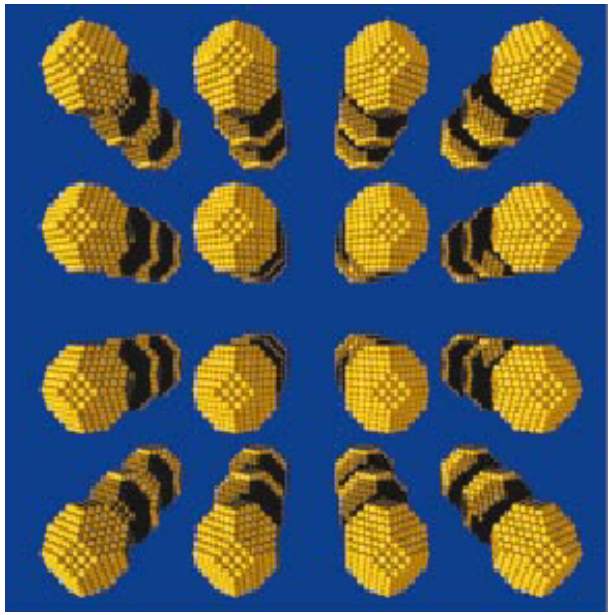

Whetten, R. L. et al. *Acc. Chem. Res.* **1999**, *32*, 397

Nanoparticles – the core

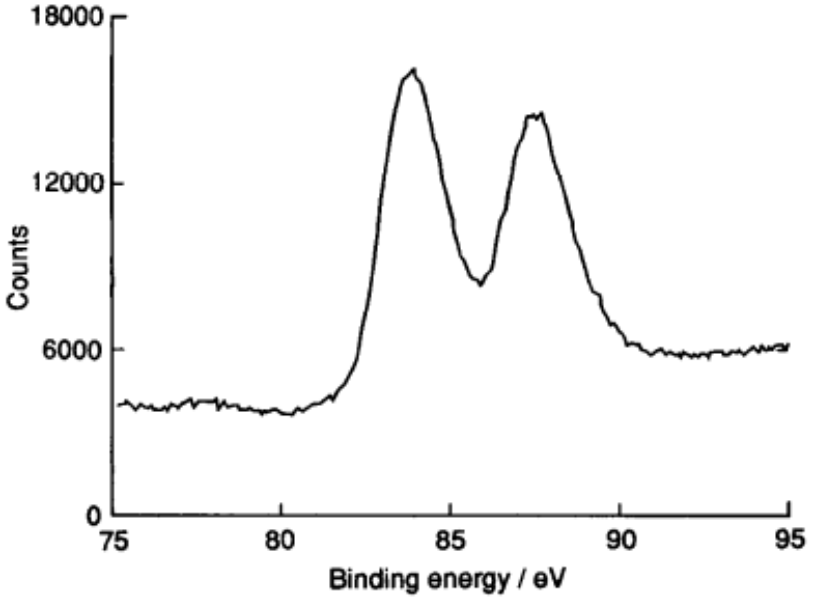

Fig. 3 XPS spectrum of the nanoparticles showing the Au $4f_{7/2}$ and $4f_{5/2}$ doublet with binding energies of 83.8 and 87.5 eV respectively. These are typical values for Au^0.

Nanoparticles - the monolayer

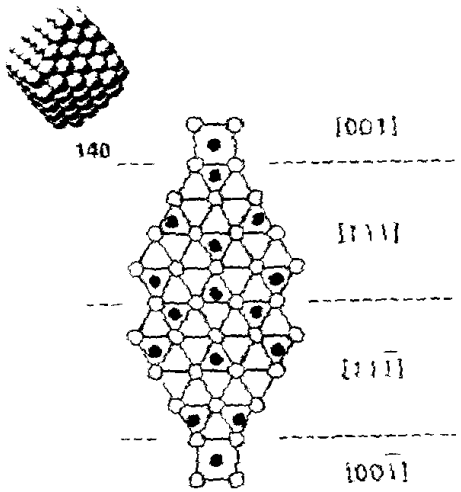

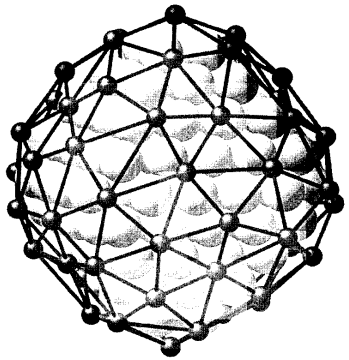

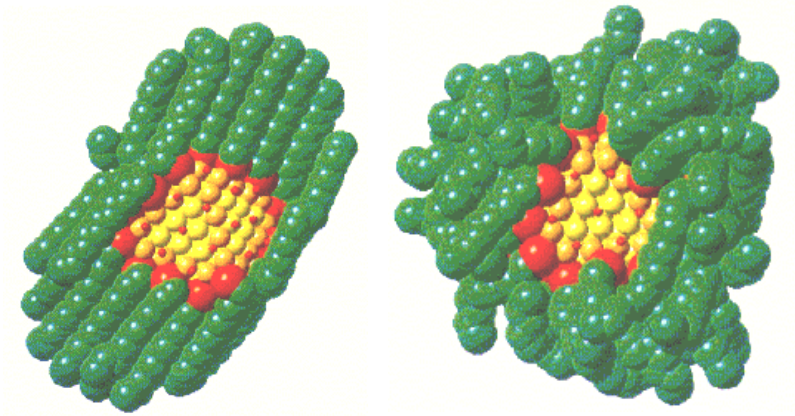

200 K

350 K

$Au_{140}(C_{12}H_{25}S)_{62}$

W. D. Luedtke, U. Landman *J. Phys. Chem.* **1996**, *100*, 13323; *J. Phys. Chem. B* **1998**, *102*, 6566

Au-NPs

Structure of a Thiol Monolayer–Protected Gold Nanoparticle at 1.1 Å Resolution

Science **2007**, *318*, 430.

Pablo D. Jadzinsky,[1,2]* Guillermo Calero,[1]* Christopher J. Ackerson,[1]†
David A. Bushnell,[1] Roger D. Kornberg[1]‡

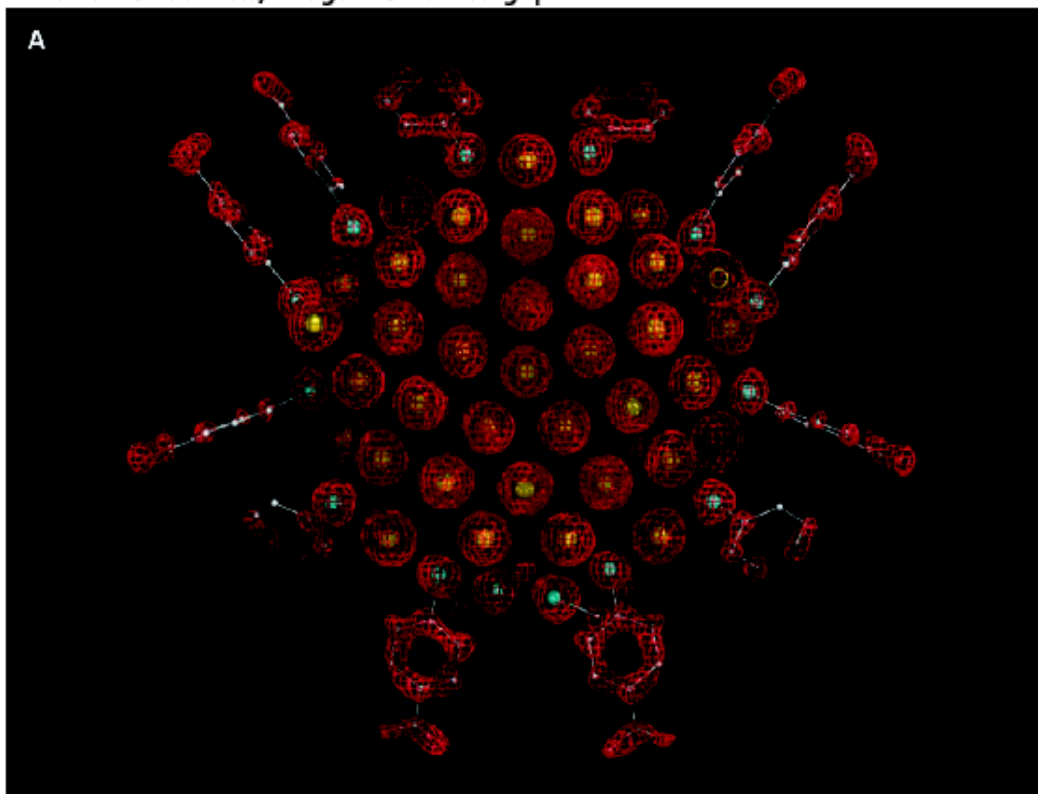

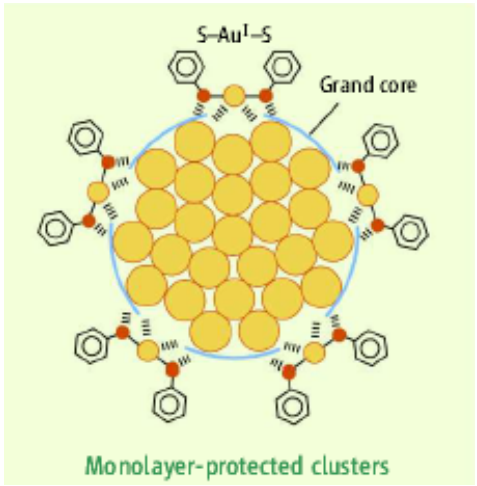

Fig. 1. X-ray crystal structure determination of the Au102(p-MBA)44 nanoparticle. (A) Electron density map(redmesh)andatomic structure (gold atoms depicted as yellow spheres, and p-MBA shown as framework and with small spheres [sulfur in cyan, carbon in gray, and oxygen in red]).

Au-NPs

Structure of a Thiol Monolayer–Protected Gold Nanoparticle at 1.1 Å Resolution

Science **2007**, *318*, 430.

Pablo D. Jadzinsky,[1,2]* Guillermo Calero,[1]* Christopher J. Ackerson,[1]†
David A. Bushnell,[1] Roger D. Kornberg[1]‡

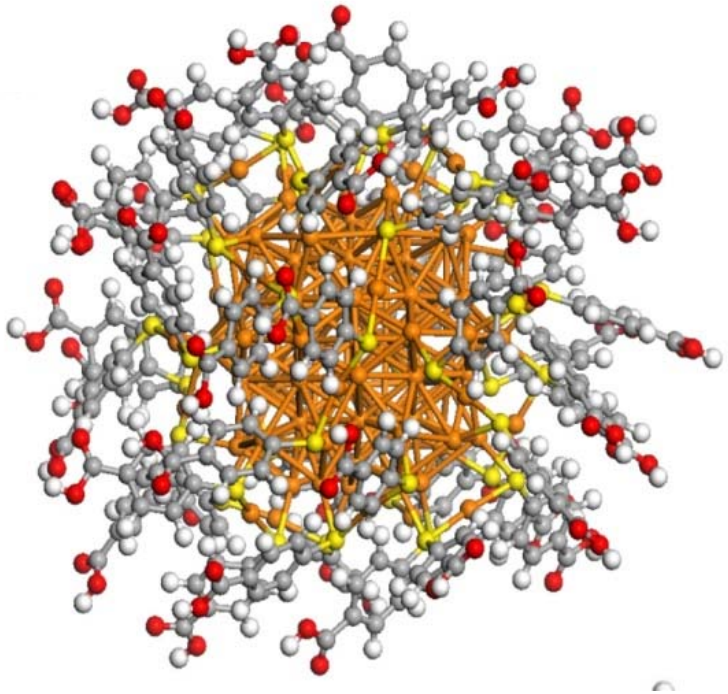

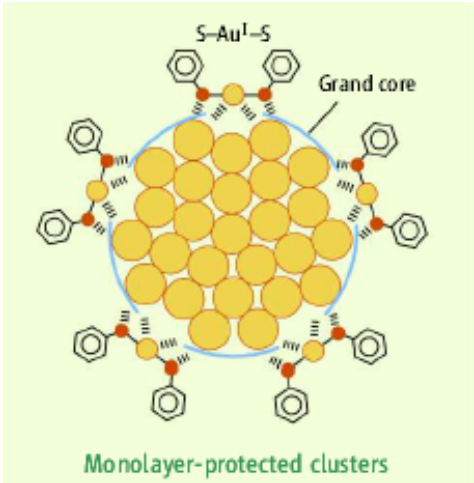

Fig. 1. X-ray crystal structure determination of the Au102(p-MBA)44 nanoparticle. (A) Electron density map(redmesh)andatomic structure (gold atoms depicted as yellow spheres, and p-MBA shown as framework and with small spheres [sulfur in cyan, carbon in gray, and oxygen in red]).

Structure of a thiol monolayer-protected Gold Nanoparticle at 1.1 Å resolution

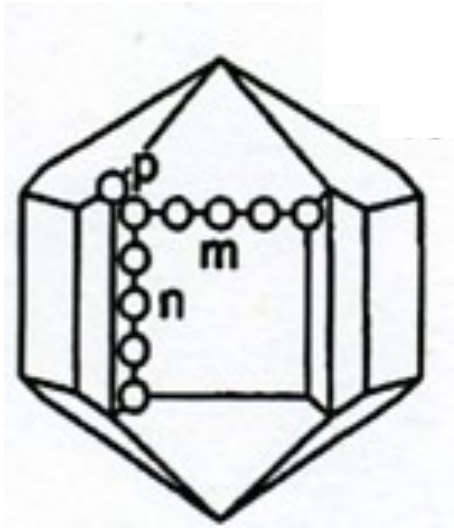

MD (m,n,p)

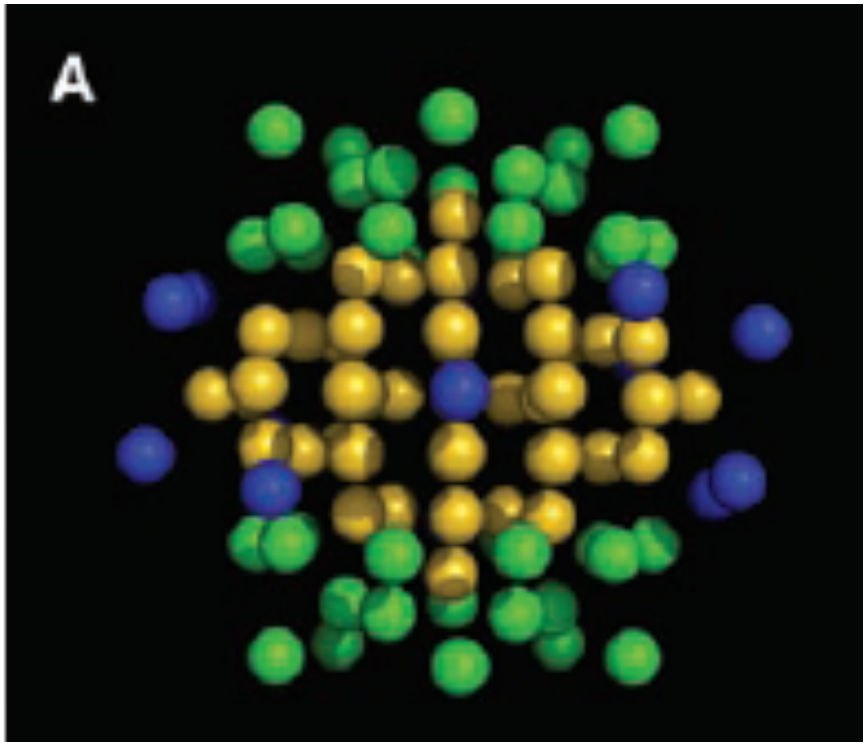

Fig.A: Packing of gold atoms in the nanoparticle. (A) MD (2,1,2) in yellow, two 20-atom“caps” at the poles in green, and the 13-atom equatorial band in blue.

Structure of a thiol monolayer-protected Gold Nanoparticle at 1.1 Å resolution

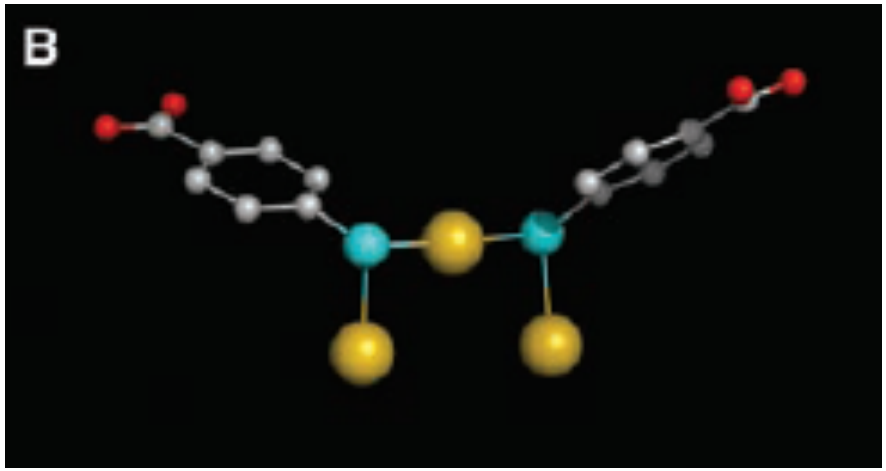

Example of two p-MBAs interacting with three gold atoms in a bridge conformation, here termed a staple motif. Gold atoms are yellow, sulfur atoms are cyan, oxygen atoms are red, and carbon atoms are gray.

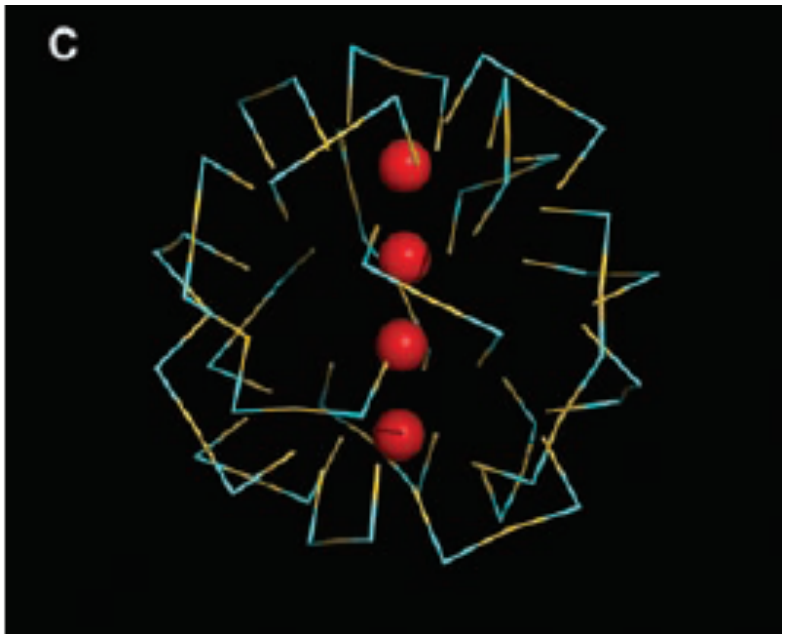

Distribution of staple motifs in the surface of the nanoparticle. Staple motifs are depicted symbolically, with gold in yellow and sulfur in cyan. Only the gold atoms on the axis of the MD are shown (in red).

Structure of a thiol monolayer-protected Gold Nanoparticle at 1.1 Å resolution

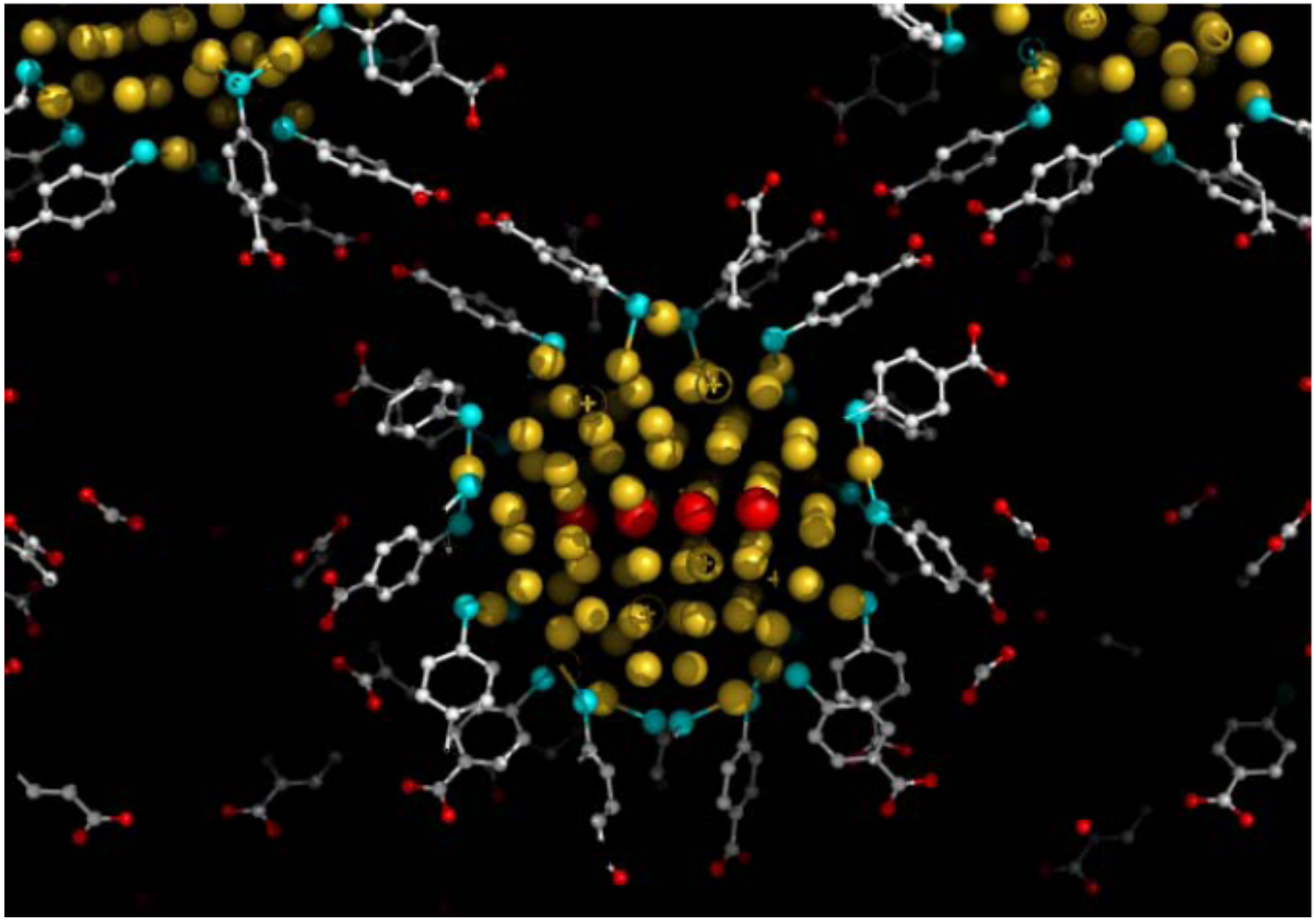

View of the crystal structure showing interparticle interaction mediated throughhydrogen bonding between carboxylic acids.

Structure of a thiol monolayer-protected Gold Nanoparticle at 1.1 Å resolution

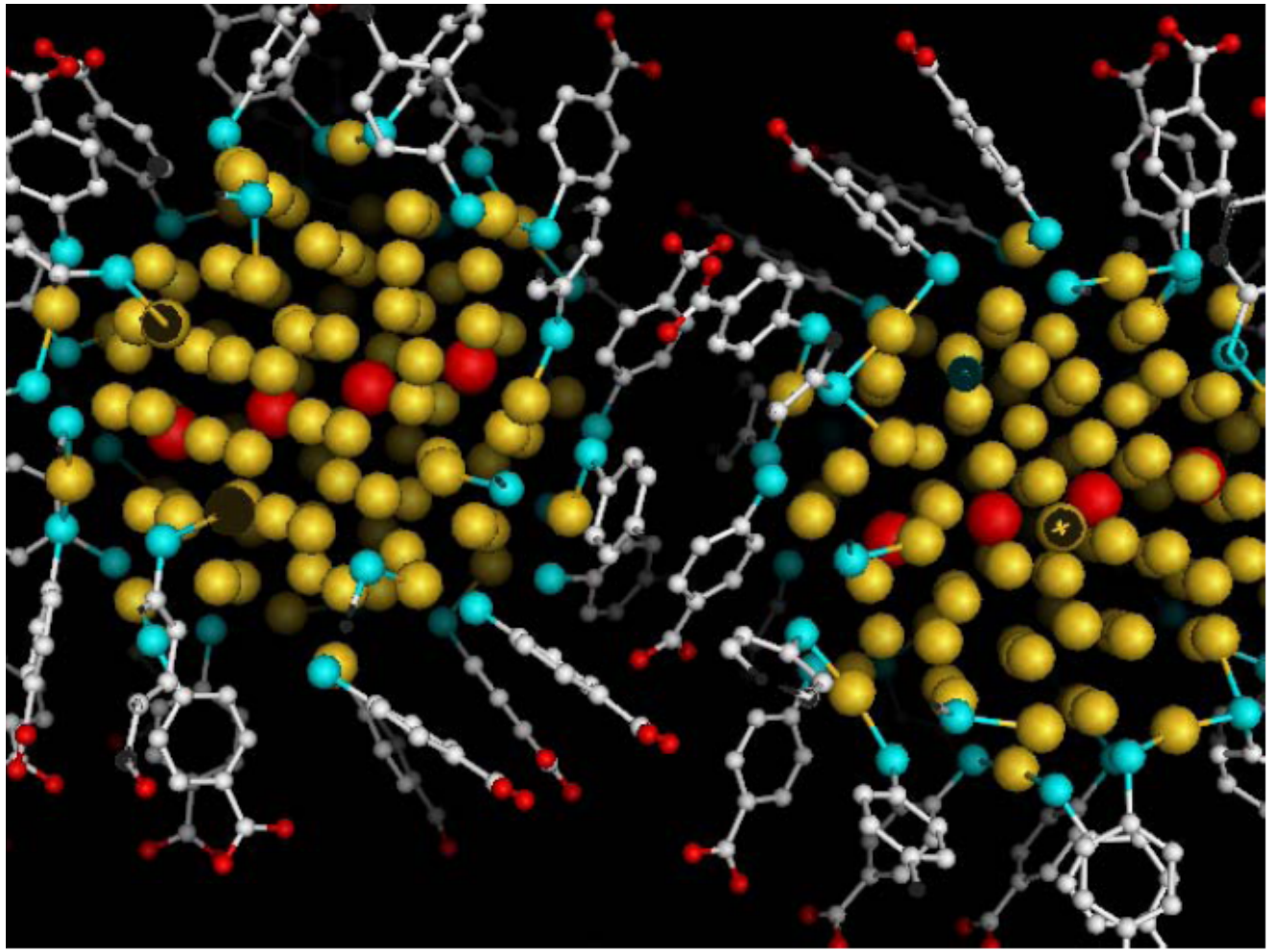

View of the crystal structure showing interparticle interactions mediated between stacked phenyl rings.

Crystal Structure of the Gold Nanoparticle [N(C8H17)4][Au25(SCH2CH2Ph)18]

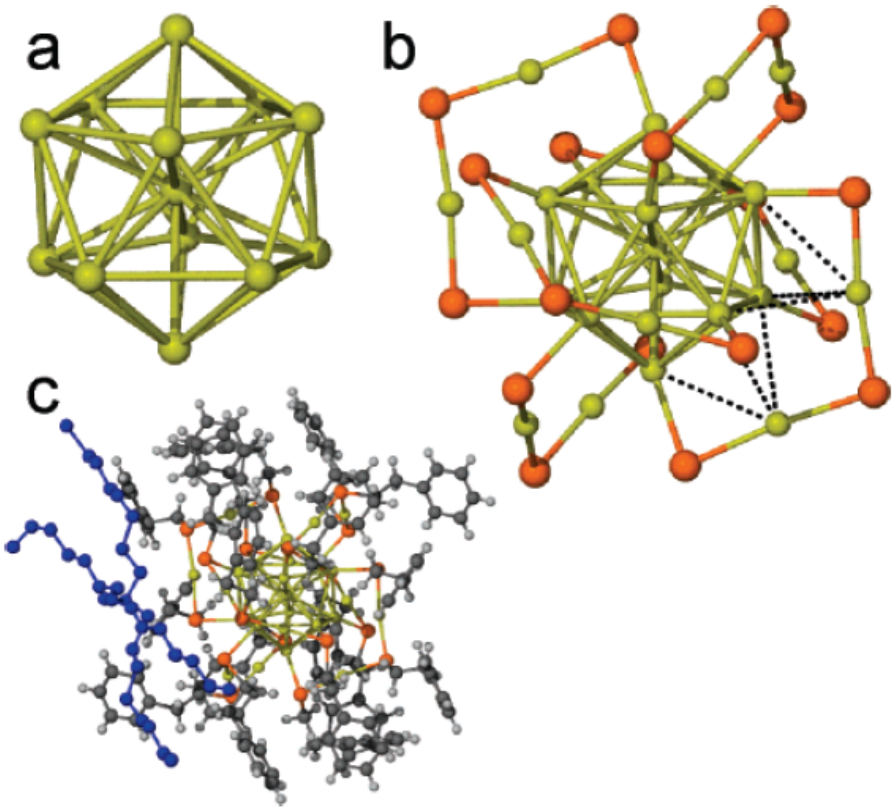

Figure 1. Breakdown of X-ray crystal structure of $[TOA^+][Au_{25}(SCH_2CH_2Ph)_{18}^-]$ as seen from [001]. (a) Arrangement of the Au_{13} core with 12 atoms on the vertices of an icosahedron and one in the center. (b) Depiction of gold and sulfur atoms, showing six orthogonal $-Au_2(SCH_2CH_2Ph)_3-$ "staples" surrounding the Au_{13} core (two examples of possible aurophilic bonding shown as dashed lines). (c) $[TOA^+][Au_{25}(SCH_2CH_2Ph)_{18}^-]$ structure with the ligands and TOA^+ cation (depicted in blue) (Legend: Gold = yellow; Sulfur = orange; Carbon = gray; Hydrogen = off-white; the TOA^+ counterion is over two positions with one removed for clarity).

M. W. Heaven, A. Dass, P. S. White, K. M. Holt, R. W. Murray **J. AM. CHEM. SOC. 2008**, 130, 3754-3755

Nanoparticles - spontaneous ordering

when monodispersed....

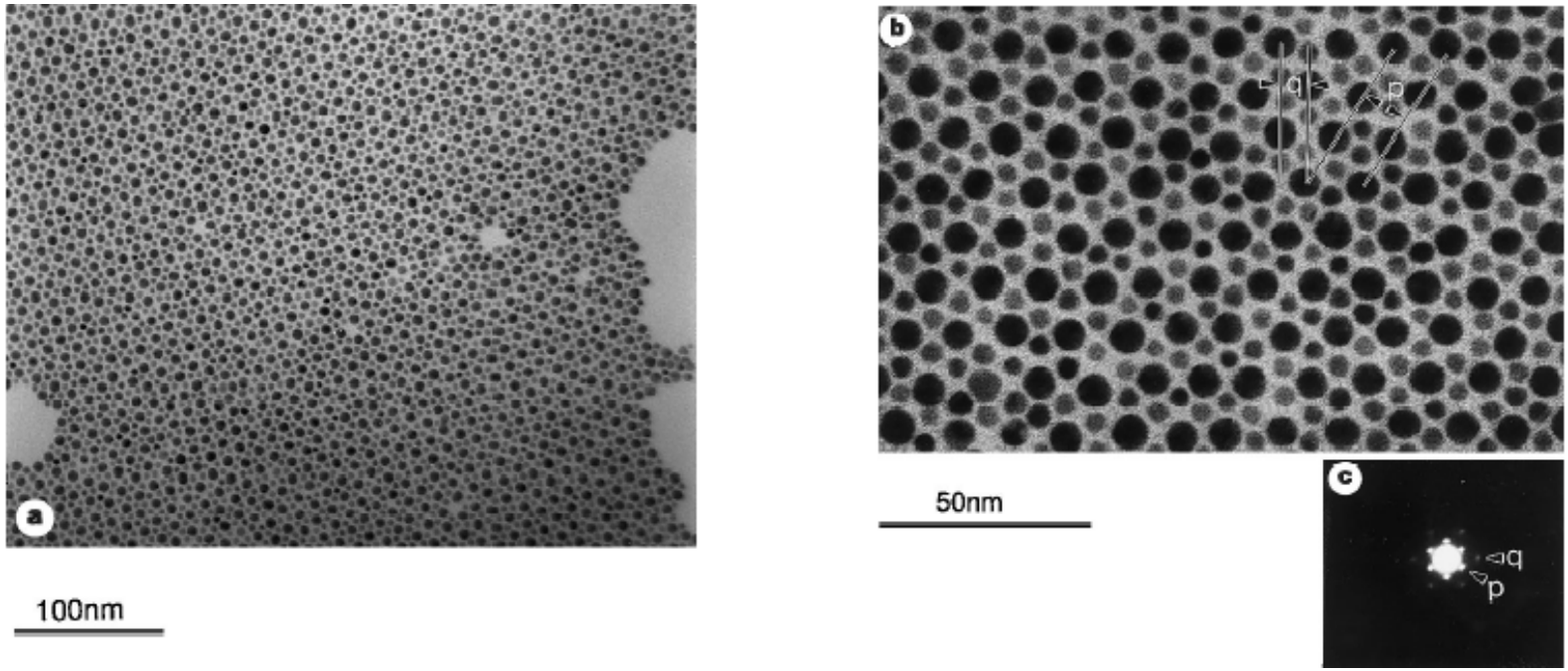

An ordered raft comprising Au nanoparticles of two distinct sizes with R_B/R_A < 0:58. Shown are electron micrographs at low (a) and higher (b) magnification. c, The low-angle superlattice electron diffraction pattern obtained from this bimodal raft structure.

C. J. Kiely, J. Fink,M. Brust, D. Bethell, D. J. Schiffrin, *Nature*, **1998**, *396*, 444.

3D alkanethiolate monolayers

Scheme 1. A Schematic 2D Representation of the RS/Au Nanoparticle Packing Structure in the Solid State[a]

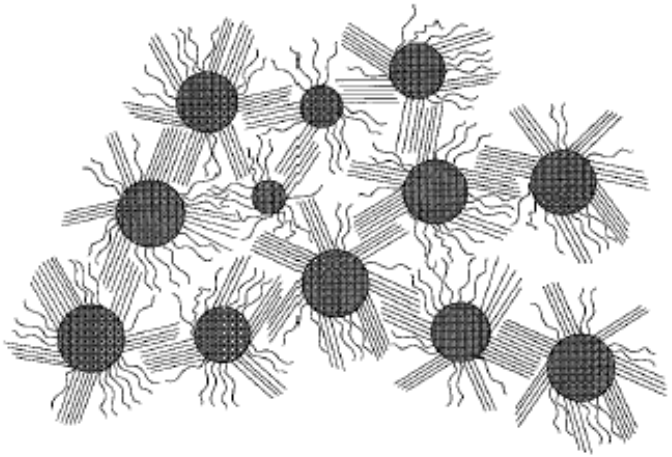

[a] In this description, *domains* or *bundles* of ordered alkylthiolate chains on a given Au particle will interdigitate into the chain domains of neighboring particles in order to compensate for the substantial decrease in the chain density which occurs toward the methyl chain end. Chains with large populations of *gauche* bonds may arise from (i) those which occupy interstitial regions in the particle lattice and cannot efficiently overlap with adjacent chains or from (ii) chains residing at domain boundaries.

Scheme 2. The Types of Chain Dynamic Processes Suggested by the ^{2}H NMR Line Shapes of the Deuterated $C_{18}S$/Au Nanoparticles[a]

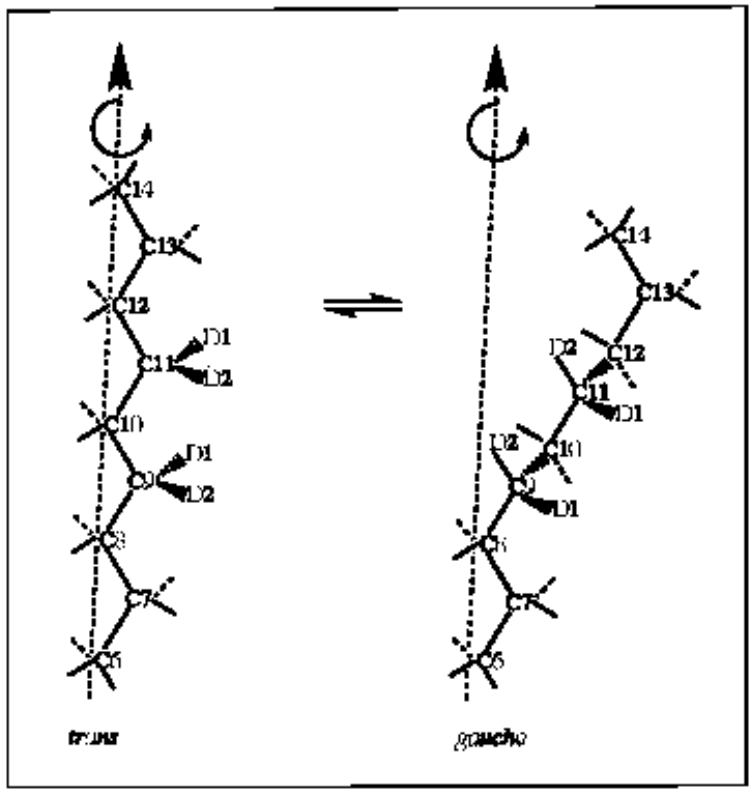

[a] These processes involve *trans-gauche* bond isomerization and pseudorotational motion of individual chain segments about the long axis of the alkanethiolate molecule.

A. Badia, L. Cuccia, L. Demers, F. Morin, B. R. Lennox, *J. Am. Chem. Soc.*, **1997**, *119*, 2682.

3D alkanethiolate monolayers

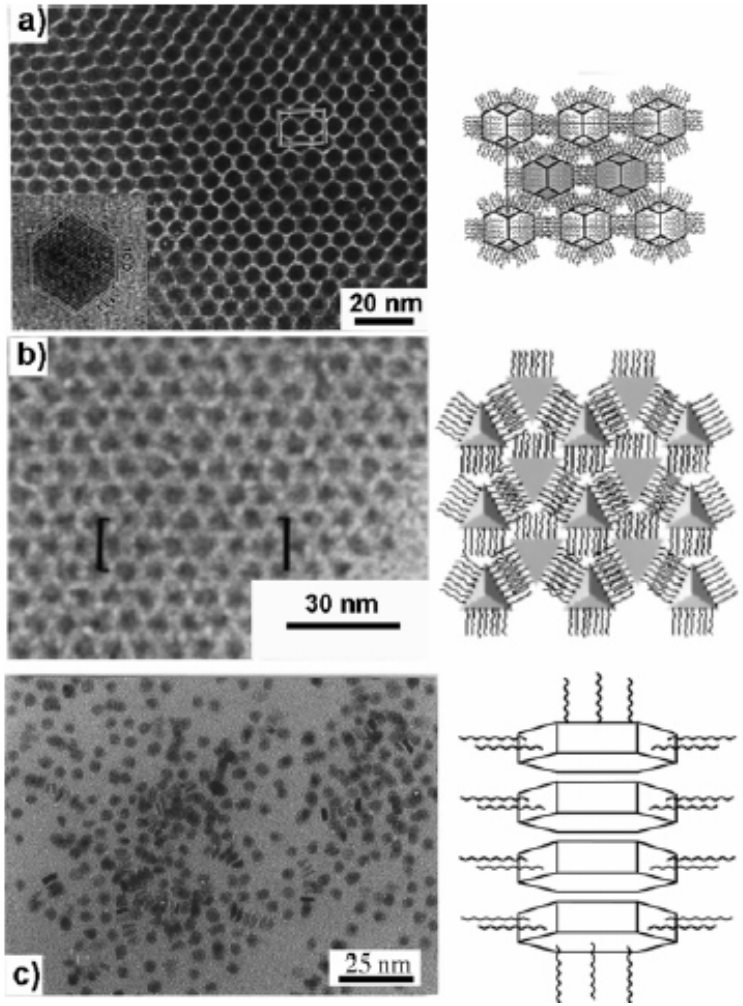

Figure 11. (a) (Left) TEM image of a face-centered, cubicpacked, array of silver nanoparticles, passivated with a dodecanethiolate monolayer, with a truncated octahedral morphology (see inset). (Right) Representation of the proposed packing of the particles via interdigitation of the bundled alkyl chains on each face. (b) (Left) TEM image of a monolayer of self-assembled silver tetrahedra passivated with dodecanethiolates. The bracketed area most closely matches the proposed model.

Langmuir **1998**, *14*, 17−30

Alkanethiolate Gold Cluster Molecules with Core Diameters from 1.5 to 5.2 nm: Core and Monolayer Properties as a Function of Core Size

Michael J. Hostetler,[†] Julia E. Wingate,[†] Chuan-Jian Zhong,[‡] Jay E. Harris,[†] Richard W. Vachet,[†] Michael R. Clark,[†] J. David Londono,[§] Stephen J. Green,[†] Jennifer J. Stokes,[†] George D. Wignall,[§] Gary L. Glish,[†] Marc D. Porter,[‡] Neal D. Evans,[⊥] and Royce W. Murray*,[†]

Table 1. Size and Composition Results for Different Cluster Preparations

preparation conditions[a]	SAXS[b] R_G, nm, max/min	SAXS[c] R_{POROD}, nm	HRTEM[d] R_{TEM}, nm	TGA[e] % organic	NMR[f] CH_3, ν_{FWHM} Hz
−78°,2X,sd	1.7/0.91	0.76	—	30.7	16
0°,2X,fd	—	—	1.1	28.8	21
0°,2X,md	—	—	—	26.7	22.5
0°,2X,sd	1.7/1.0	0.89	1.1	26.2	25.5
RT,1X,fd	1.7/1.2	1.0	—	25.6	24.5
RT,4X,fd	1.7/1.1	0.94	—	24.9	26
RT,2X,sd	1.6/1.2	0.96	—	24.5	27
RT,2X,fd	—	—	—	23.7	25.5
60°,2X,sd	1.4/1.2	0.98	—	24.1	29
90°,2X,sd	—	—	1.1	23.2	32
RT,1/2X,fd	1.6/1.4	1.2	1.2	19.4	37
RT,1/3X,fd	1.8/1.6	1.4	1.4	16.9	45
RT,1/4X,fd	2.1/2.0	1.7	2.0	12.8	53
RT,1/6X,fd	2.9/2.5	2.2	2.2	9.3	126[g]
RT,1/8X,fd	—	—	—	10.4	124[g]
RT,1/10X,fd	—	—	2.4	6.2	144[g]
RT,1/12X,fd	—	—	2.6	11.9	163[g]

[a] Code for preparation conditions: (*a*,*b*,*c*), where *a* represents the temperature at which the reduction was carried out, *b* represents the RSH:$AuCl_4^-$ molar ratio before reduction, and *c* represents the rate of reductant addition (fd, 10 s; md, 2 m; sd, 15 m). [b] SAXS results for Au core radius determined from Guinier plot. [c] SAXS results from Porod plot. [d] HRTEM results, average Au core size from analysis of histogram of HRTEM images. [e] TGA for thermal loss of alkanethiolate fraction of clusters. [f] Proton NMR linewidths. [g] CH_3 ^{1}H NMR signal obscured; the CH_2 resonance was used instead for these clusters.

Nanoparticles - caracterization

TEM

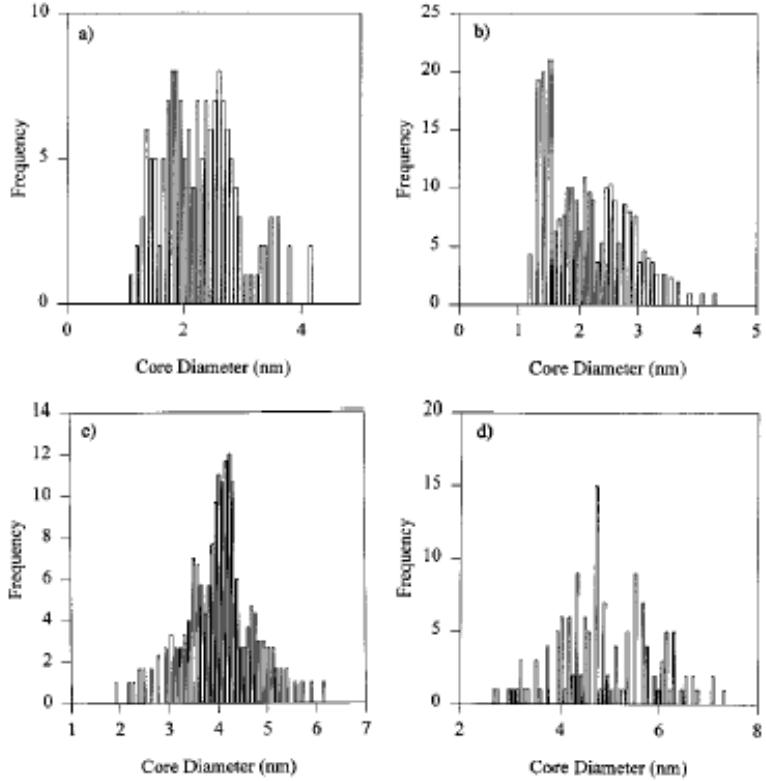

Figure 2. Size histograms (a and d are for films shown in Figure 1): (a) (0°,2X,fd); (b) (0°,2X,sd); (c) (RT,1/4X,fd); (d) (RT, 1/6X,fd).

NANOPARTICELLE - characterization

Table 2. Results from Modeling of Gold Core Sizes, Shapes, and Alkanethiolate Coverages, and of Size-Dependent T_2 Broadening of Proton NMR of CH_3 Resonances

#atoms (shape)[a]	R_{CORE}, nm	#surface atoms/ %defect/area nm^2	calc TGA %organic/ %coverage/#chains	calc R_{TOTAL}, nm	calc NMR ν_{FWHM}, Hz
79 (TO^+)	0.65	60/60%/8.30	33.0/63%/38	2.6	15
116 (TO^-)	0.71	78/61%/11.36	31.8/68%/53	2.6	16
140 (TO^+)	0.81	96/50%/11.43	27.9/55%/53	2.7	17
201 (TO)	0.87	128/47%/15.22	26.5/55%/71	2.8	18
225 (TO^+)	0.98	140/43%/15.19	24.4/51%/71	2.9	19
309 (CO)	1.1	162/52%/19.64	23.3/57%/92	3.0	22
314 (TO^+)	1.0	174/41%/19.46	22.9/52%/91	3.0	20
459 (TO^+)	1.2	234/36%/24.34	20.2/49%/114	3.1	23
586 (TO)	1.2	272/35%/28.94	19.1/50%/135	3.2	24
807 (TO^+)	1.4	348/31%/34.86	17.1/47%/163	3.3	27
976 (TO^-)	1.5	390/31%/40.02	16.4/48%/187	3.4	28
1289 (TO)	1.6	482/27%/47.22	14.9/46%/221	3.5	32
2406 (TO)	2.0	752/22%/69.86	12.2/43%/326	3.9	42
2951 (TO^+)	2.2	876/21%/79.44	11.4/42%/371	4.1	47; 94[b]
4033 (TO)	2.4	1082/19%/97.00	10.3/42%/453	4.3	55; 110[b]
4794 (TO^+)	2.6	1230/18%/108.28	9.7/41%/506	4.4	61; 122[b]
6266 (TO)	2.8	1472/16%/128.66	8.9/41%/601	4.7	70; 140[b]

[a] CO = cuboctahedron; TO = ideal truncoctahedron (all sides equal); TO^+ = truncoctahedron in which $(0 < n - m \leq 4)$, where n is the number of atoms between (111) facets and m is the number of atoms between (111) and (100) facets; TO^- = truncoctahedron in which $(-4 \leq n - m < 0, m > 1)$. [b] The second value is the calculated linewidth for the methylene peak.

NANOPARTICELLE - characterization

NMR

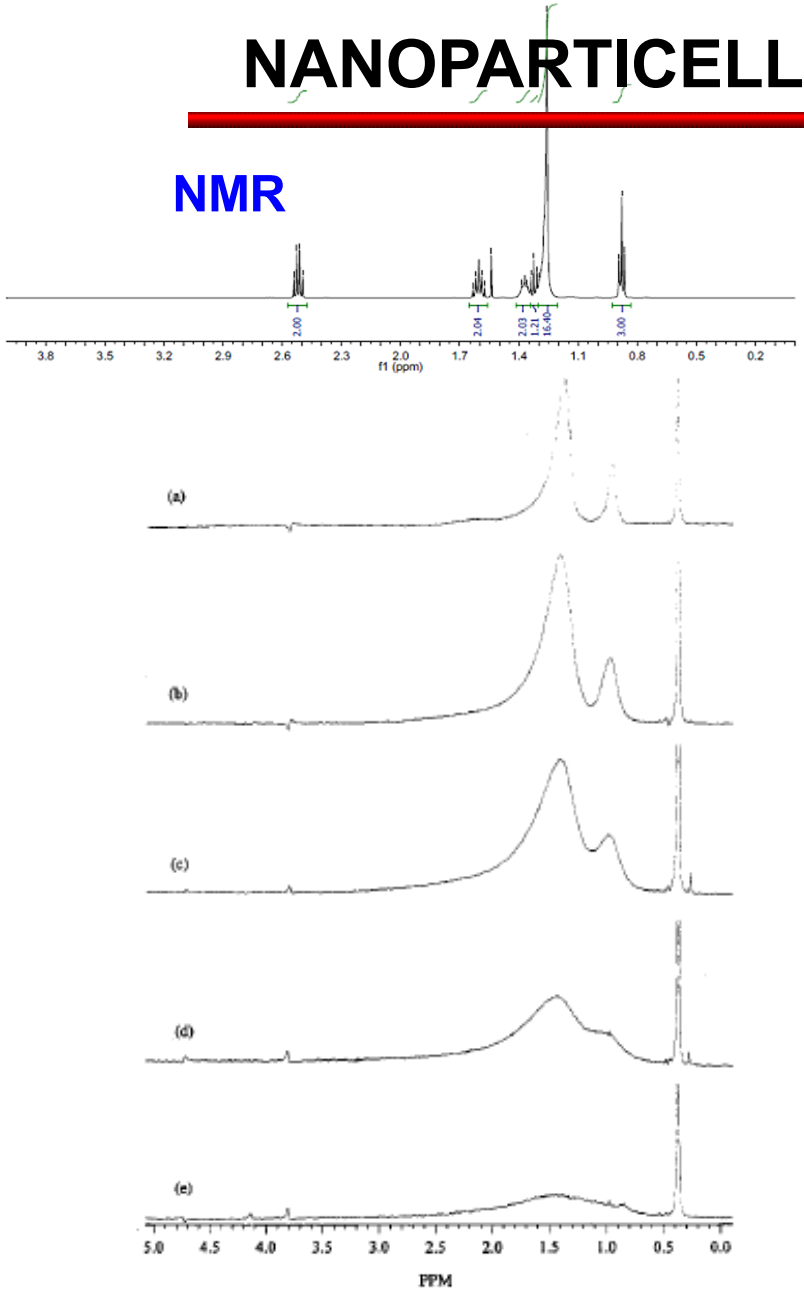

Figure 5. The ^{1}H NMR spectra (C_6D_6) of dodecanethiolate-protected Au clusters. Each spectrum was Fourier transformed using a line broadening of 1 Hz: (a) (−78°,2X,sd); (b) (90°,2X,sd); (c) (RT,1/3X,fd); (d) (RT,1/4X,fd); (e) (RT,1/12X,fd).

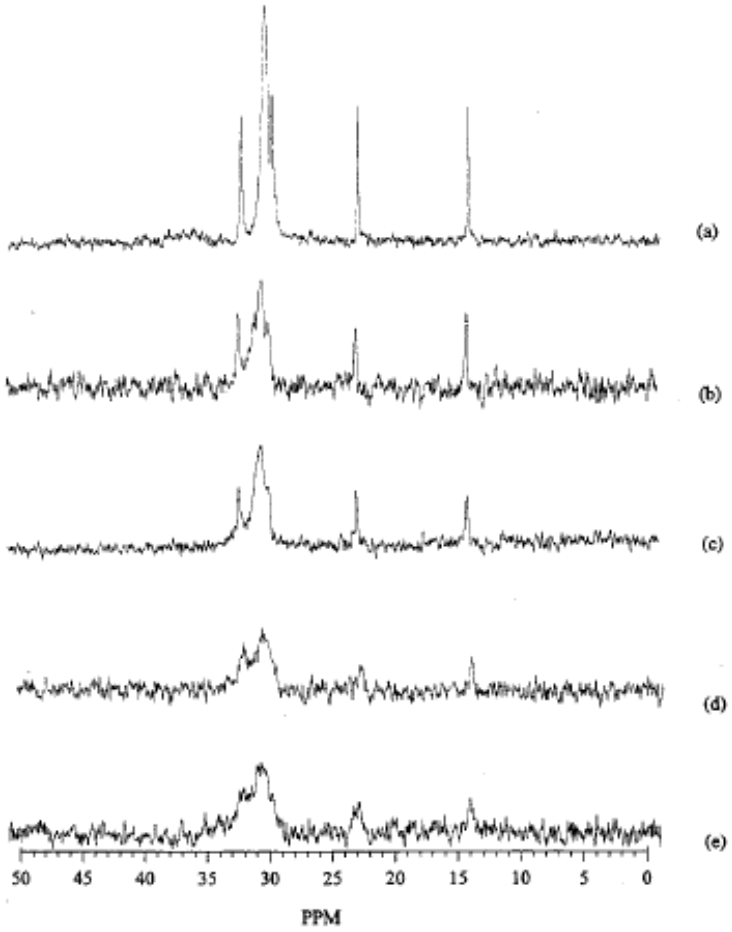

Figure 4. The ^{13}C NMR spectra (C_6D_6) of dodecanethiolate-protected Au clusters. Each spectrum was Fourier transformed using a line broadening of 3 Hz: (a) (−78°,2X,sd); (b) (90°,2X,sd); (c) (RT,1/3X,fd); (d) (RT,1/4X,fd); (e) (RT,1/6X,fd).

NANOPARTICELLE - characterization

UV-Vis

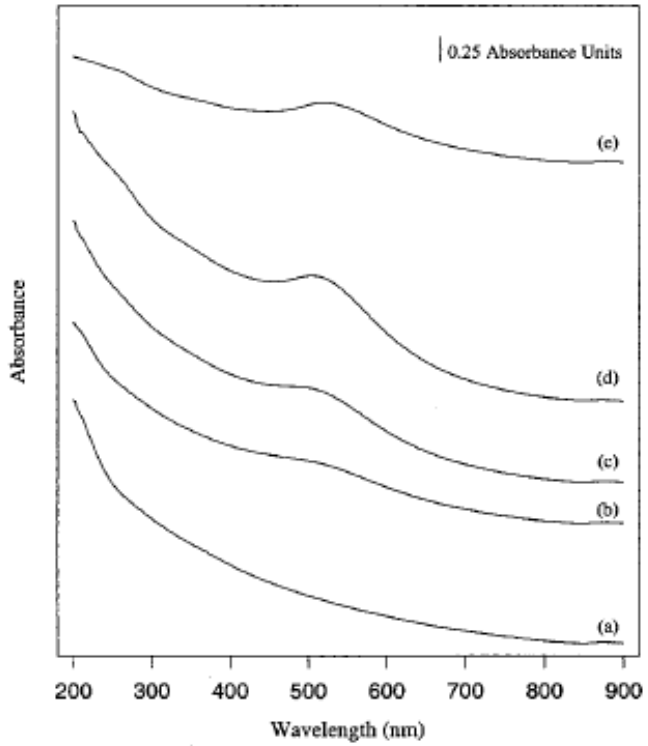

Figure 7. The UV/vis spectra (hexane) of dodecanethiolate-protected Au clusters: (a) (−78°,2X,sd), C = 3×10^{-6} M, MW = 3.4×10^4 amu; (b) (90°,2X,sd), C = 2×10^{-6} M, MW = 5.5×10^4 amu; (c) (RT,1/3X,fd), C = 4×10^{-7} M, MW = 2.3×10^5 amu; (d) (RT,1/4X,fd), C = 2×10^{-7} M, MW = 5.5×10^5 amu; (e) (RT,1/12X,fd), C = 9×10^{-8} M, MW = 1.1×10^6 amu.

MPCC12

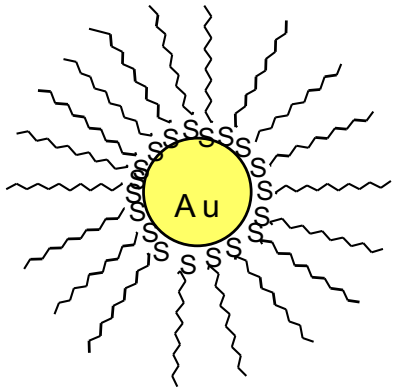

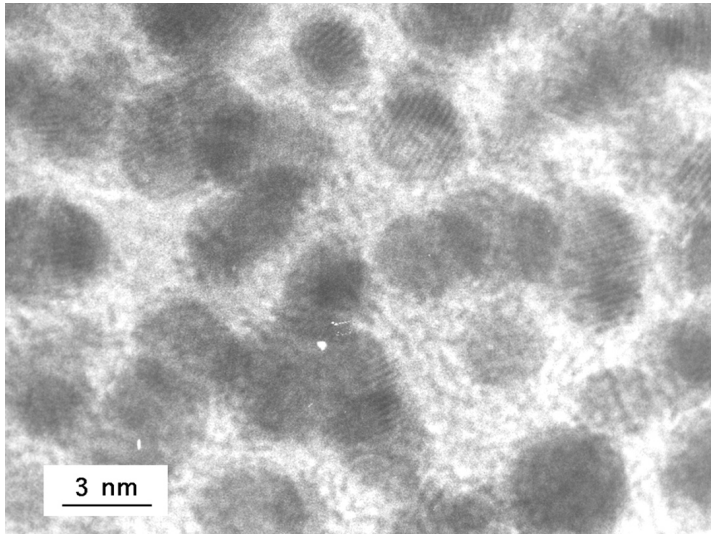

HRTEM

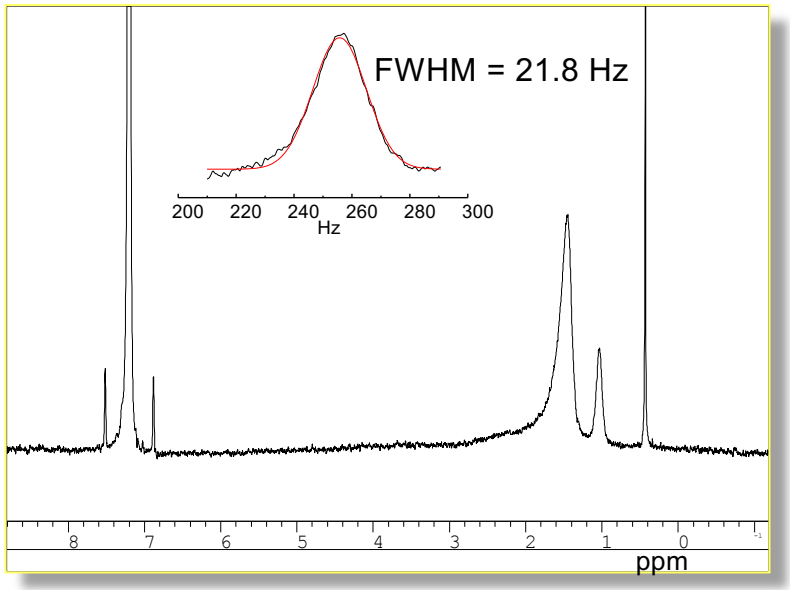

^{1}H NMR (250 MHz, C_6D_6)

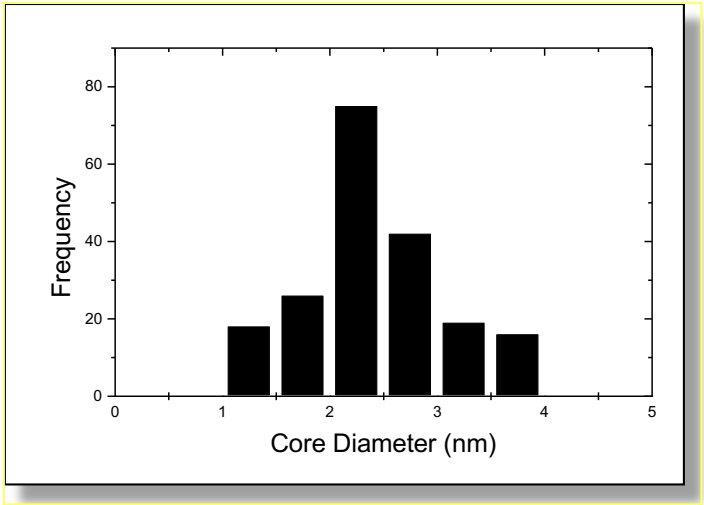

Core size histogram: core diameter 2.2 ± 0.4 nm

MPC-C12

$Au_{116}(SR)_{50}$ (MW=)

MPC-C12 - TGA Analysis

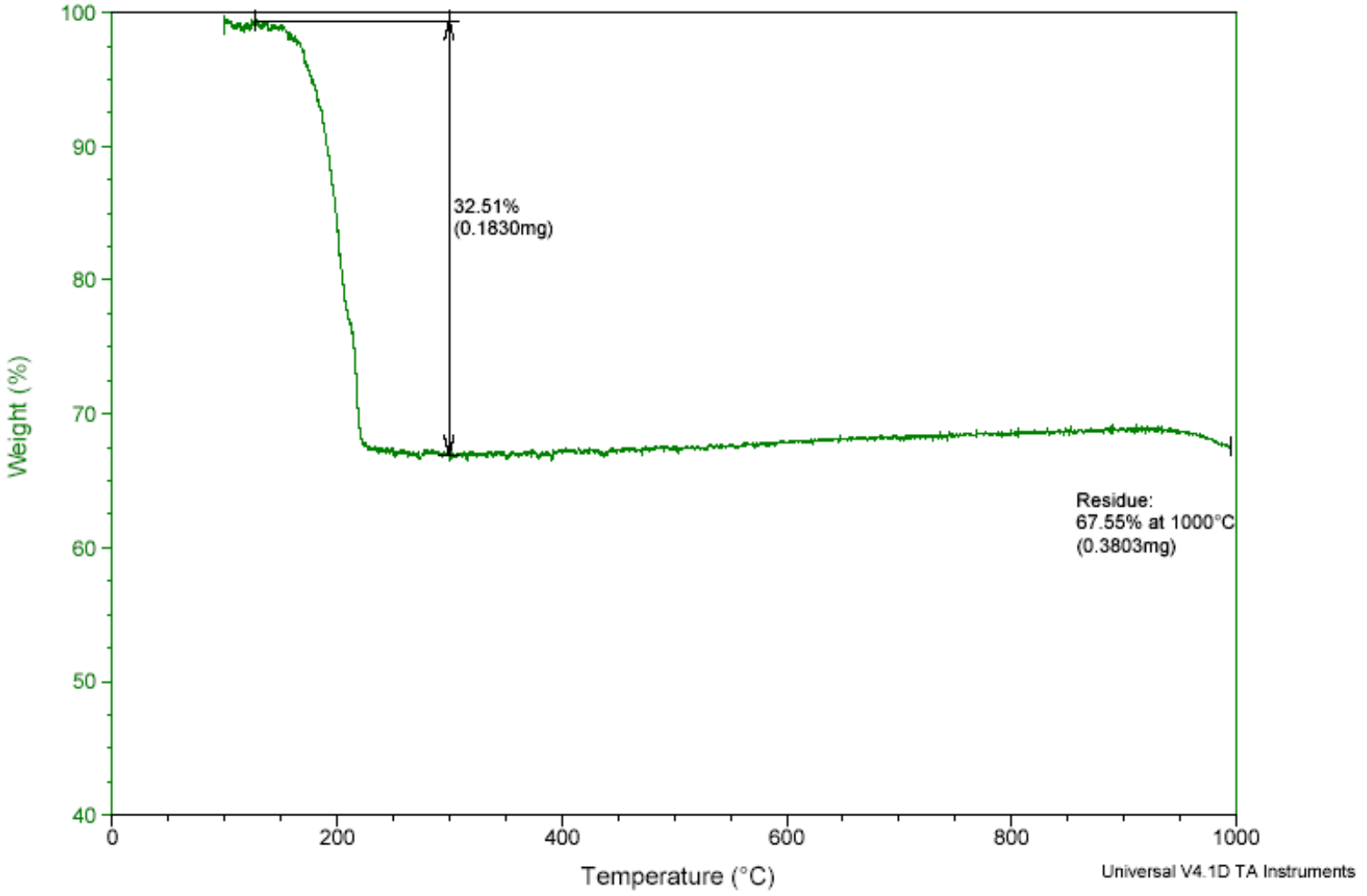

Water soluble nanoparticles

tiopronin

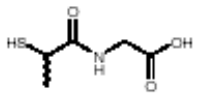

11

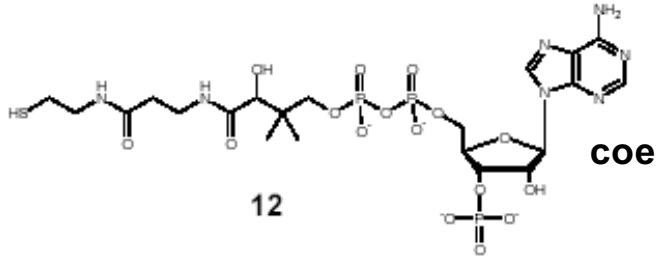

12

coenzyme A

13

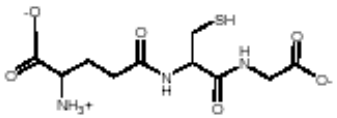

14 glutathione

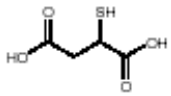

15

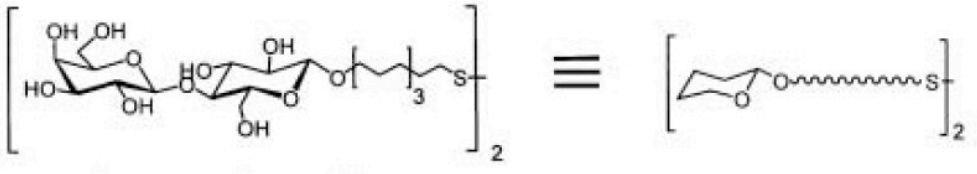

Lactose neoglycoconjugate

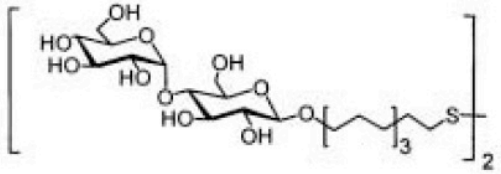

Maltose neoglycoconjugate

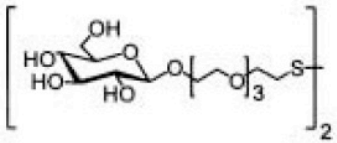

Glucose neoglycoconjugate

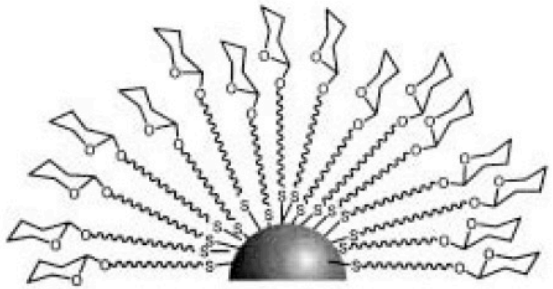

lacto-GNP
malto-GNP
gluco-GNP

Water soluble nanoparticles

$PEG_{5000}SH$

21

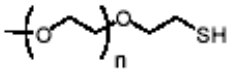

22a n = 1
22b n = 2
22c n = 3

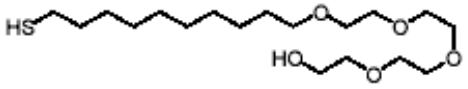

23

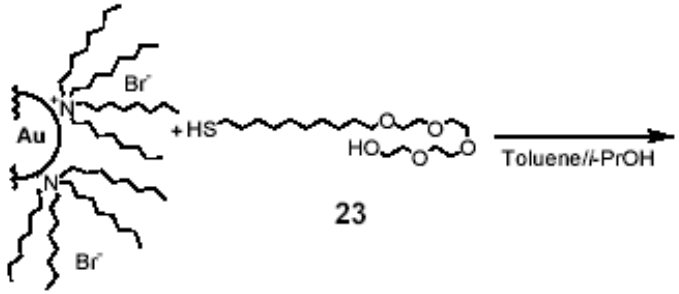

25

23

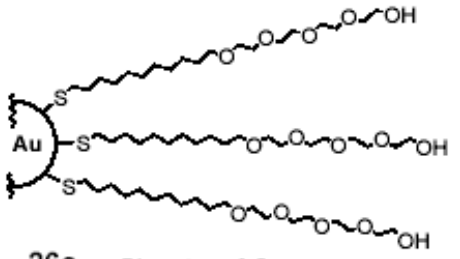

26a Diametro > 3.5 nm

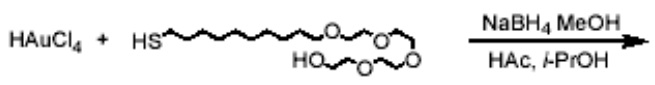

23

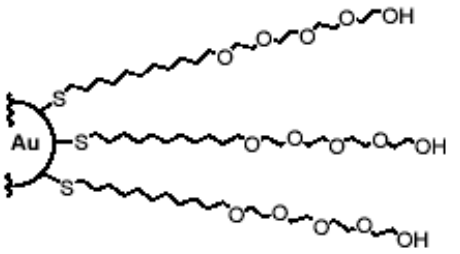

26b Diametro < 3.5 nm

Water soluble nanoparticles

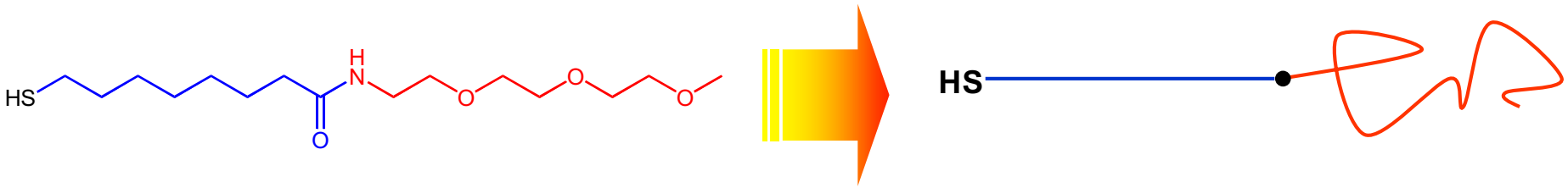

The hydrocarbon chain ensures the formation of a compact and tidy monolayer near the surface of the nanoparticle metal core

The polyether chain, even of short length, ensures MPCs solubility in water and polar solvents

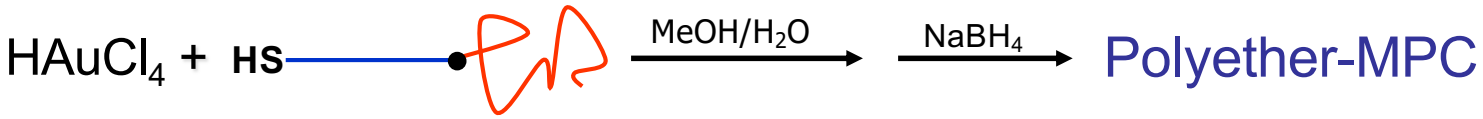

Homogeneous phase synthesis

Quantitative conversion of $HAuCl_4$

Diameter of the gold core 1.5 - 4.2 nm

Strong influence of the reduction rate

Pengo, P; Polizzi, S.; Battagliarin, M.; Pasquato, L.; Scrimin, P. *J. Mater. Chem.* **2003**, *13*, 2471-2478.

MPC-C8-TEG Characterization

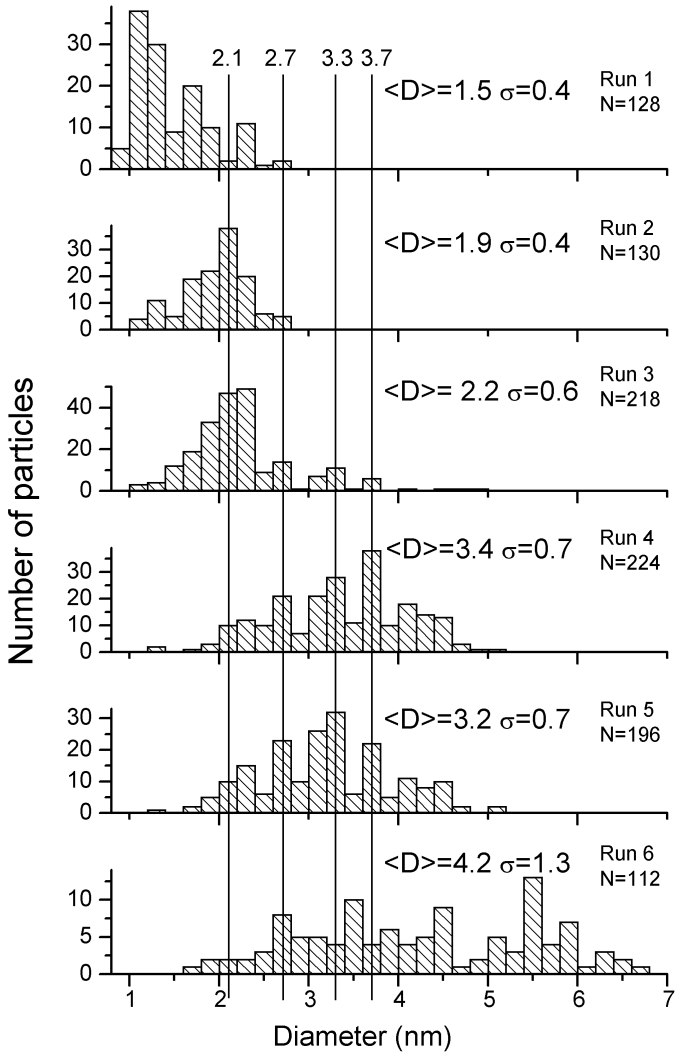

Increasing Gold / thiol ratio

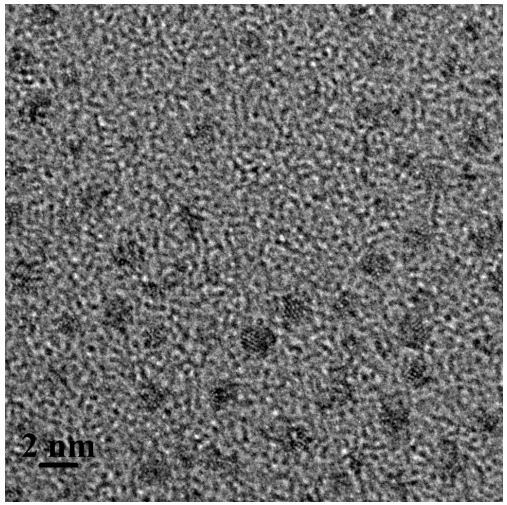

TEM image of MPCs obtained with a 1/3 gold/thiol molar ratio, $NaBH_4$ added in 10 sec.

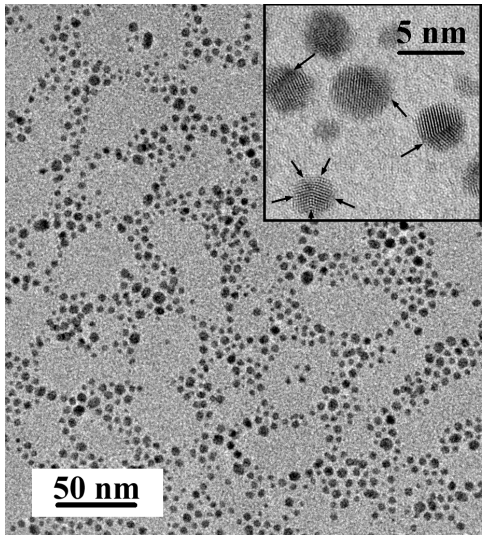

TEM image of MPCs obtained with a 3/1 gold/thiol molar ratio, adding $NaBH_4$ in 30 minutes

Thiolate Ligands for Synthesis of Water-Soluble Gold Clusters

C. J. Ackerson, P. D. Jadzinsky, R. D. Kornberg **J. AM. CHEM. SOC. 2005**, 127, 6550-6551

Table 1. Water-Soluble Thiolates and Their Ability to Passivate Gold Clusters

compound name	published synthesis	diameter (nm)[k]	soluble product	stability	synthetic method[a]	behavior in HD–PAGE gel
3-mercaptopropionic acid	ref 21	undetermined[j]	yes	days to weeks	Brust	did not enter matrix in HD or LD−PAGE[i]
4-mercaptobutyric acid	no	4.0 ± 1.2	yes	weeks	Brust	not tested
3-mercapto-1,2-propanediol	ref 14[b]	4.7 ± 1.2	yes	days	Brust	single diffuse band in HD−PAGE
cysteine	ref 12[c]	1.6 ± 0.3	yes	days	Brust[f]	entered gel matrix as single band; stalled; single band in LD−PAGE
methionine	no	2.4 ± 1.0	yes	weeks	Hutchison	did not enter matrix in HD or LD−PAGE
thiomalate	ref 13[d]	2.1 ± 1.4	yes	weeks	Brust	single tight band surrounded by large halo
2-mercaptobenzoic acid	no	2.1 ± 0.9	yes	minutes	Brust	did not enter matrix in HD or LD−PAGE
3-mercaptobenzoic acid	no	1.6 ± 0.6	yes	days	Brust	did not enter matrix; single band in LD−PAGE
4-mercaptobenzoic acid	ref 7[e]	1.8 ± 0.4	yes	months	Brust	2 tight bands
tiopronin	ref 9	1.9 ± 0.7	yes	months	Brust[f]	single diffuse pink band in HD or LD−PAGE
selenomethionine	no	1.6 ± 0.4	yes	days	Hutchison	did not enter matrix in HD or LD−PAGE
1-thio-β-D-glucose	no	2.1 ± 0.5	yes[g]	months	Brust[f]	single band in LD−PAGE
glutathione	ref 8	1.4 ± 0.4	yes	months	Brust	5 bands
ITCAE pentapeptide[h]	no	1.4 ± 0.4	yes	days	Hutchison	not tested

[a] Brust synthesis was in 1:1 water:methanol with a 3:1 thiolate:gold ratio. Typical concentrations were 10 mM gold and 30 mM thiolate. A 5-fold molar excess of $NaBH_4$ in a volume of water ~10% of the reaction volume was added to complete the cluster formation. Reactions denoted Hutchison were performed as described (ref 5). [b] A 1:1 ratio of thiolate:Au(III) and a 9-fold BH_4^- excess. [c] Cystine was used as the starting material to create cysteine MPCs. [d] Highest organothiolate:Au(III) ratio used was 5:2, with equimolar $NaBH_4$ to $HAuCl_4$, likely resulting in incomplete reduction. [e] A 1.8:1 thiolate:Au(III) ratio was used. [f] These compounds failed to form soluble products in 1:1 water:methanol, but did so under similar conditions in 6:1 methanol:acetic acid. [g] This compound formed product that remained in suspension following low-speed centrifugation, indicating cluster formation, but failed to redissolve after methanol precipitation; this product was not repeatably precipitable in methanol, but could be purified from starting materials by gel filtration and, otherwise, behaved as a stable water-soluble MPC. [h] The pentapeptide had the sequence Ile-Thr-Cys-Ala-Glu. [i] LD−PAGE was a standard 12% SDS−PAGE gel. [j] Particles form aggregates within which individual particle diameters cannot be measured. [k] See Supporting Information for images, histograms, and further analysis.

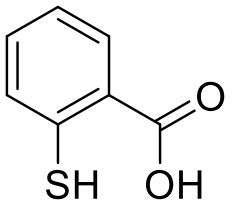

2-mercaptopropionic acid

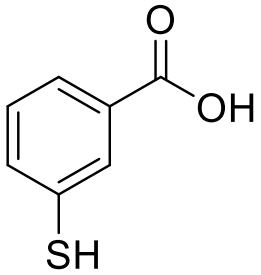

3-mercaptopropionic acid

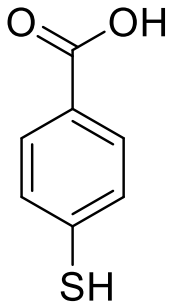

4-mercaptopropionic acid